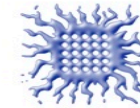




NICA Days 2023



Belgrade, Serbia
02-03
10.23

Global event characterization in heavy-ion collisions



Grigory Feofilov
(*St. Petersburg State University*)

02.10.2023, 14:00, 45m

Vinča Institute of Nuclear Sciences, Belgrade, SERBIA
"Belgrade Panorama" conference hall

https://indico.jinr.ru/e/nica_days2023

Literature

- C.Y. Wong, [Introduction to High-Energy Heavy-Ion Collisions](#), World Scientific, 1994
- L. P. Csernai, [Introduction to Relativistic Heavy-Ion Collisions](#), 1994 (book is freely available as pdf)
- E. Shuryak, [The QCD vacuum, hadrons, and superdense matter](#), World Scientific, 2004
- Yagi, Hatsuda, Miake, [Quark-Gluon Plasma](#), Cambridge University Press, 2005
- R. Vogt, [Ultrarelativistic Heavy-ion Collisions](#), Elsevier, 2007
- W. Florkowski, [Phenomenology of Ultra-Relativistic Heavy-Ion Collisions](#), World Scientific, 2010
- S. Sarkar, H. Satz and B. Sinha, [The physics of the quark-gluon plasma](#), Lecture notes in physics, Volume 785, 2010

Talk layout

- Introduction.
- What are we colliding.
- Multiplicity, p_T , transverse energy
and energy density in AA collisions
- Reaction plane and Event plane
- Selection of central events
- Conclusion

✓ Introduction

” Relativistic nuclear physics” : a bit of History



A.M. Baldin

1971: the 1st relativistic nuclear beams with an energy of 4.2 AGeV at the synchrotron at the LHE, JINR. One of the 1st studies

of nuclear effects in the high energy interactions off nuclei

A.M. Baldin et al.

Sov.J. Nucl.Phys.18,41 (1973)

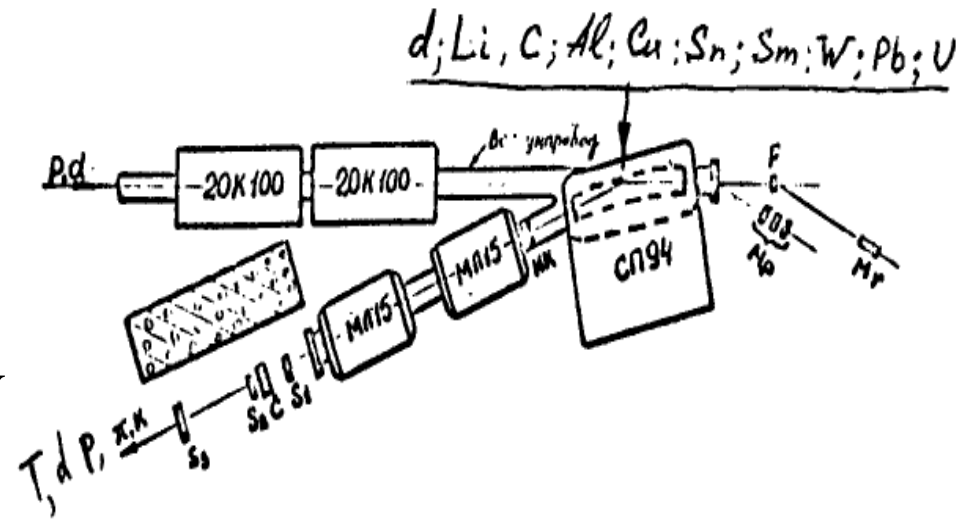


Fig. 2 Experimental layout

A.M. Baldin , "Heavy Ion Interactions at High Energies", report at AIP Conf. Proc. 26, 621 (1975)

➔ BEVALAC(1972), SPS(1976), RHIC(2000), LHC(2009)

...a bit of History...

HADRONIC INTERACTIONS OF HIGH ENERGY COSMIC-RAY OBSERVED BY EMULSION CHAMBERS

C.M.G. LATTES

Instituto de Fisica Gleb Wataghin, Universidade Estadual de Campinas, Campinas, Sao Paulo, Brasil

Y. FUJIMOTO and S. HASEGAWA

Science and Engineering Research Laboratory, Waseda University, Shinjuku, Tokyo, Japan

In 1980: "...we found that the decay temperature of a fire-ball is of the order of a pion rest-energy, $m_\rho c^2$, much smaller than the participating energies in the collision..."

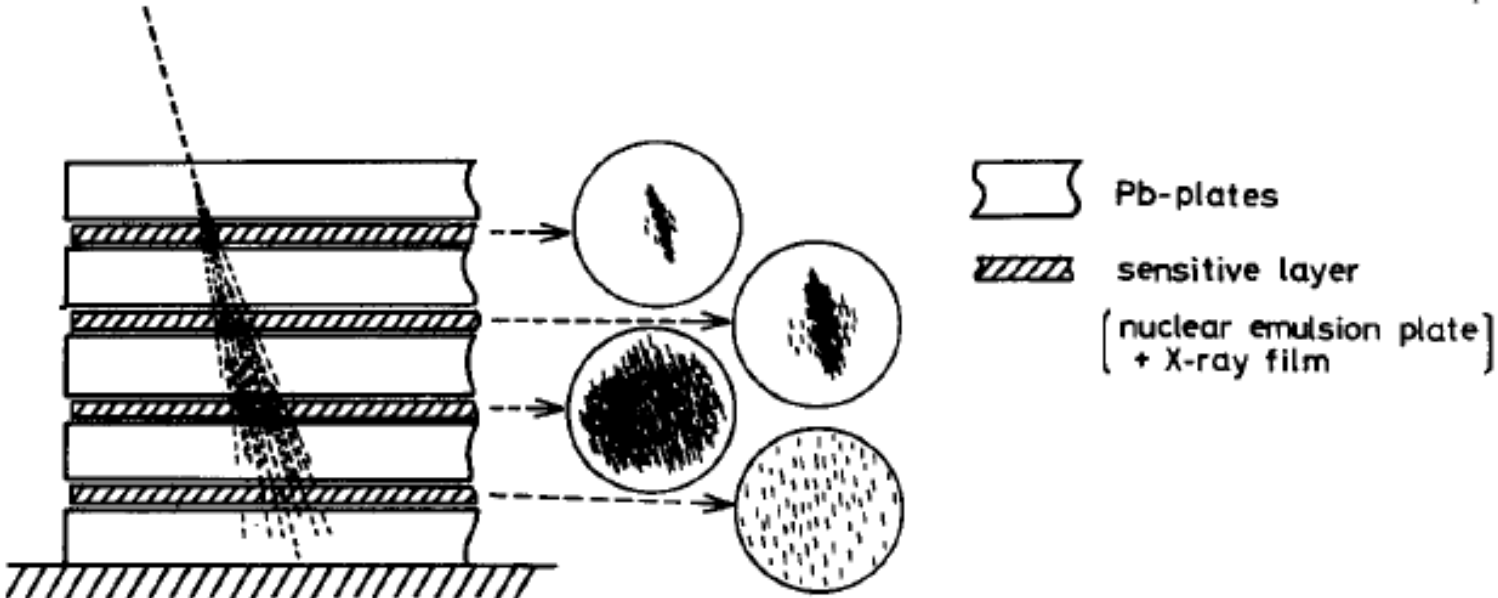


Fig. 1. Basic structure of emulsion chamber as electron shower detector.

... a bit of History: QGP

...J. C, Collins and M. J. Perry -1975, ...E.Shuryak 1978...:

Шуряк Э В "Кварк-глюонная плазма" УФН 138 327–328 (1982)

QUARK–GLUON PLASMA AND HADRONIC PRODUCTION OF LEPTONS, PHOTONS AND PSIONS

E.V. SHURYAK

Institute of Nuclear Physics, Novosibirsk, USSR

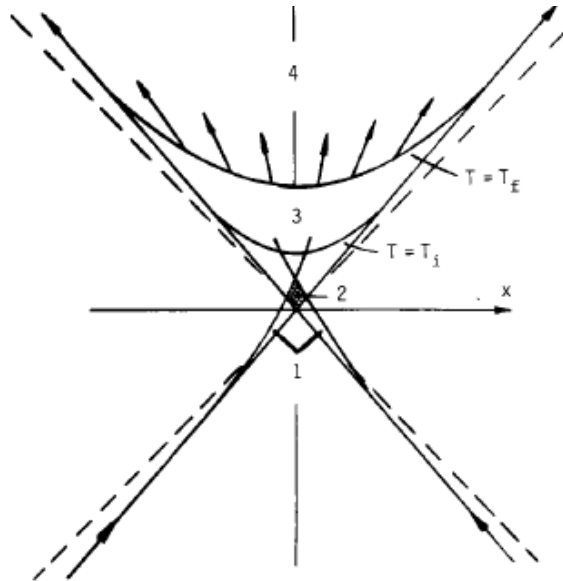


Fig. 1. The space–time picture of hadronic collisions, proceeding through the following stages: (1) structure function formation; (2) hard collisions; (3) final state interaction; (4) free secondaries.

Early expectations: QGP like an ideal gas of quarks and gluons

At very high energy density, the coupling constant of QCD becomes weak. A gas of particles should to a good approximation become an ideal gas. Each species of particle contributes to the energy density of an ideal gas as

$$\epsilon \sim \frac{\pi^2}{30} N T^4$$

where N is the number of particle degrees of freedom. At low temperatures when masses are important, only the lowest mass, strongly interacting particle degree of freedom contributes; the pion, and the energy density approaches zero as $\epsilon \sim e^{-m_\pi/T}$. For an ideal gas of pions, the number of pion degrees of freedom is three. For a QGP there are two helicities and eight colours for each gluon, and for each quark, three colours, two spins, and a quark–antiquark pair. The number of degrees of freedom is $N \sim 2 \times 8 + 4 \times 3 \times N_F$ where N_F is the number of important quark flavours, which is about three if the temperature is below the charm quark mass so that $N \sim 50$.

Relativistic heavy-ion physics: three lectures

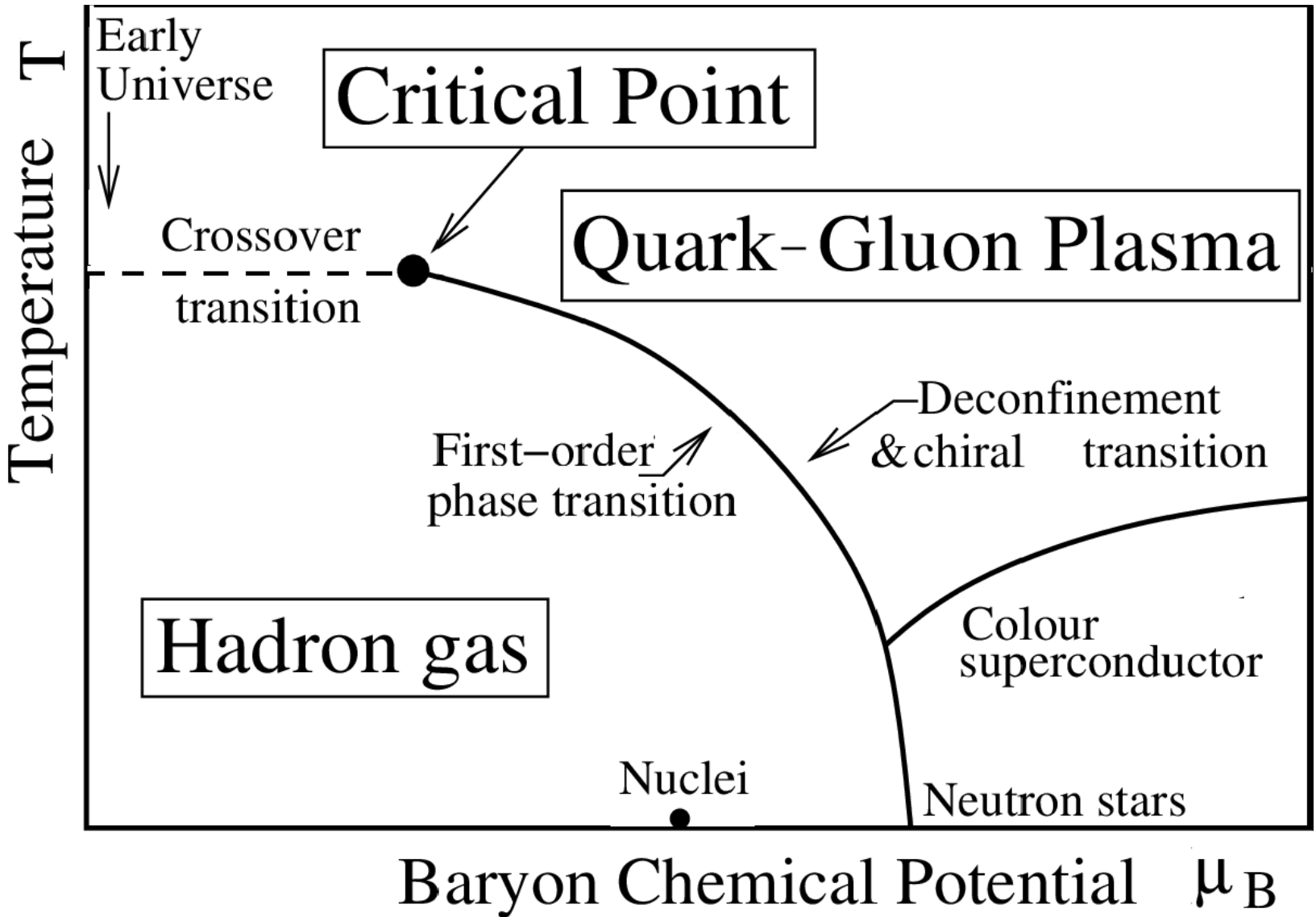
L. McLerran

Brookhaven National Laboratory, Upton, NY 11973, USA and RIKEN BNL Research Center, Brookhaven National Laboratory, Upton, NY 11973, USA

Phys. Lett. B78 (1978) 150

➤ QGP: lots of interesting questions to be answered !

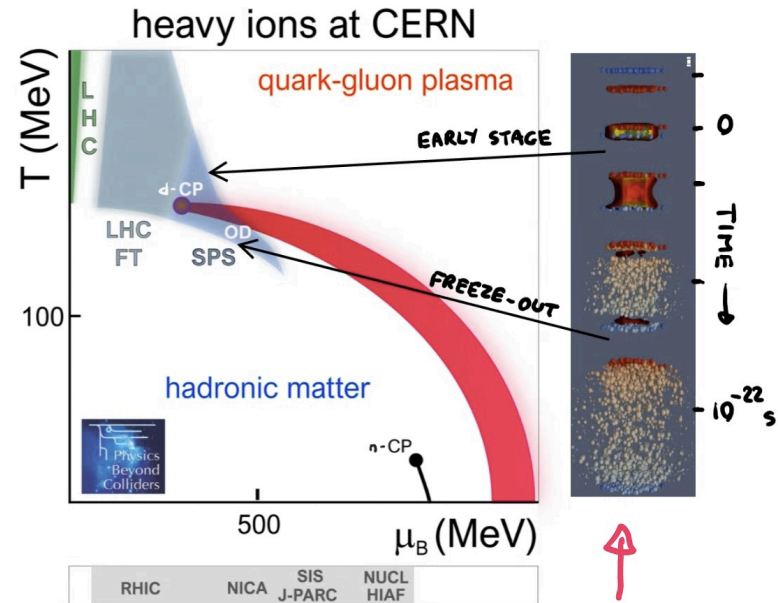
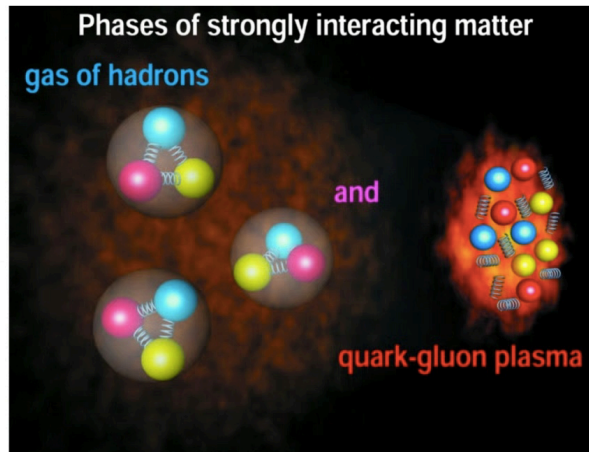
Phase diagram of strongly interacting matter



Bhalerao, Rajeev S. (2014). "Relativistic heavy-ion collisions". In Mulders, M.; Kawagoe, K. (eds.). 1st Asia-Europe-Pacific School of High-Energy Physics. CERN Yellow Reports: School Proceedings. Vol. CERN-2014-001, KEK-Proceedings-2013-8. Geneva: CERN. pp. 219-239. doi:10.5170/CERN-2014-001. ISBN 9789290833994. OCLC 801745660. S2CID 119256218.

STRONG INTERACTIONS

WHAT HAPPENS WHEN STRONGLY INTERACTING MATTER GETS HOTTER/DENSER AND ITS VOLUME CHANGES ?

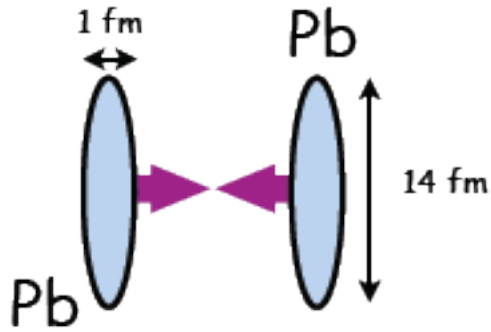


NA61/SHINE: WHAT HAPPENS IN HEAVY ION COLLISIONS?

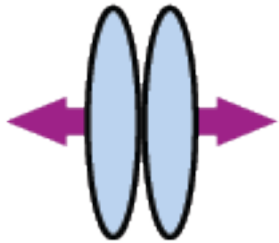
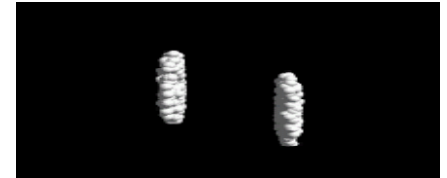
13

Slide by Marek Gazdzicki (Goethe University Frankfurt), NA61/SHINE Collaboration,
See also report by Marjan Čirković (Faculty of Physics, University of Belgrade),
“News from the NA61/SHINE”, 6 Oct, 2023, 13:30 - 14:00 CET
<https://indico.jinr.ru/event/3746/timetable/#20231004>

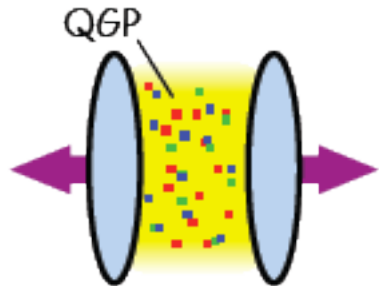
Phases of nuclear collisions



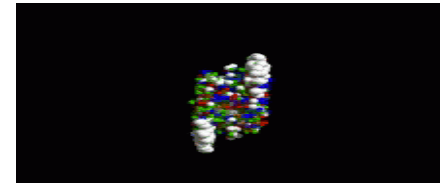
- Before collision



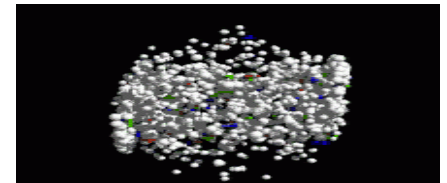
- Thermalization: ($t < 1$ fm/c) equilibrium is established



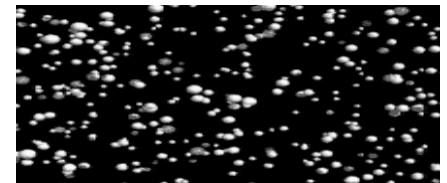
- Expansion and cooling ($t < 10-15$ fm/c)



- Chemical freeze-out: inelastic collisions cease (number of particles frozen)

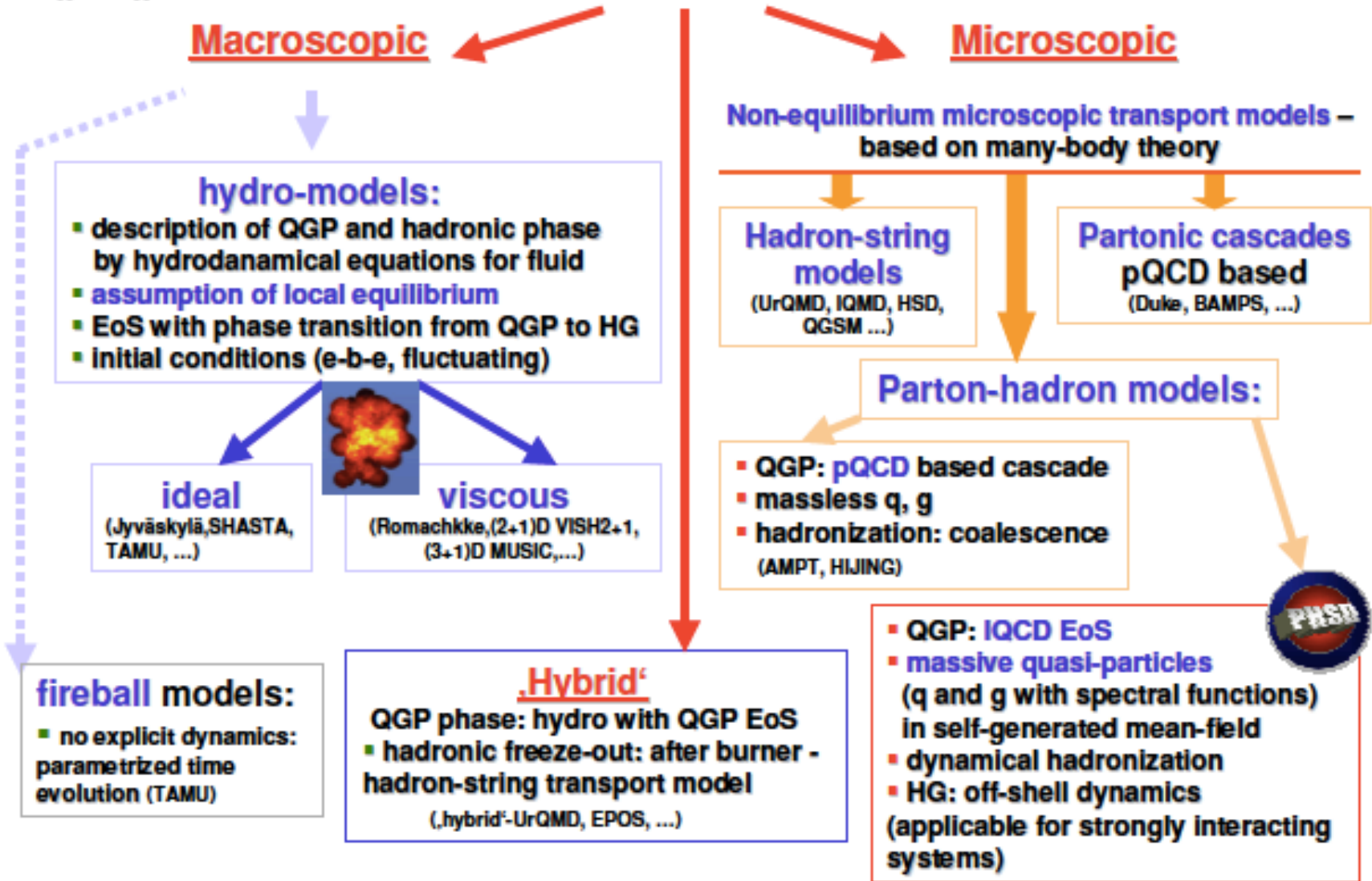


- Kinetic freeze-out: elastic collisions cease (momentum spectra frozen)





Dynamical models for HIC



Slide by Elena Bratkovskaya, “Kruger2014: The International Workshop on Discovery Physics at the LHC”, Protea Hotel Kruger Gate, South Africa, 1-5 December 2014

Nuclear-nuclear collisions: two theoretical approaches [1]

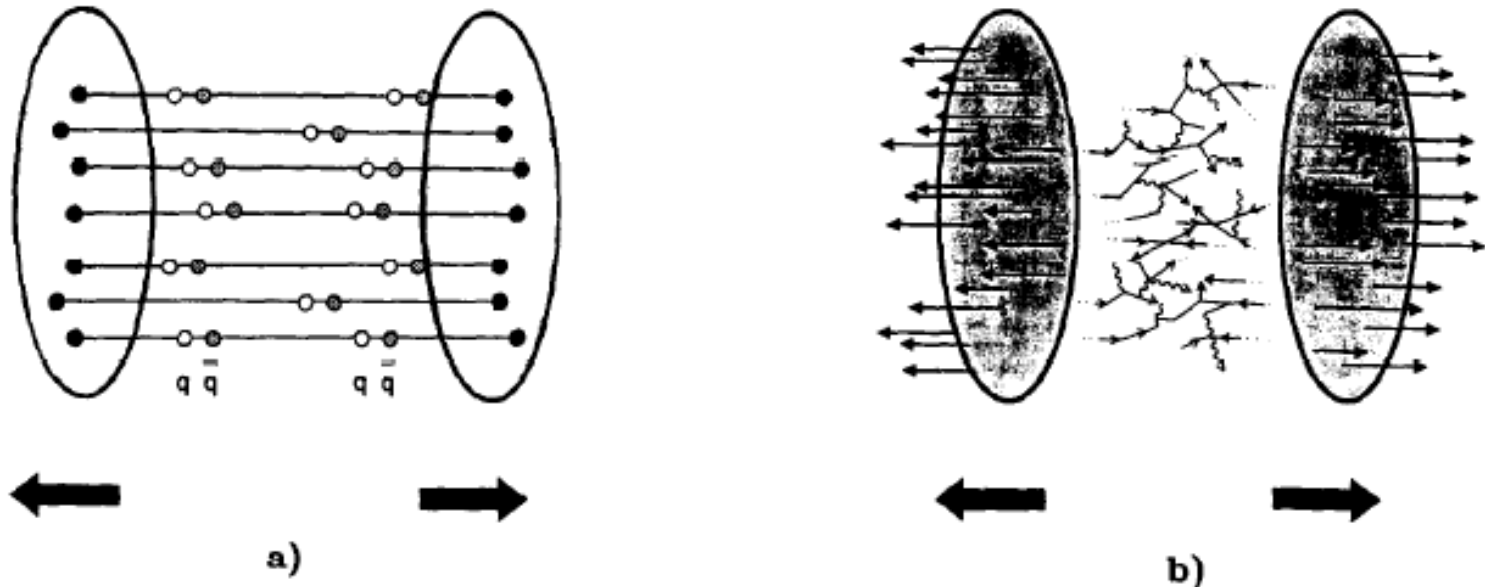


Fig. 2. (a) **String picture**: primary interactions lead to color flux tubes (strings) which break by $q\bar{q}$ production.

(b) **Parton approach**: multiple scatterings accompanied by emission and absorption of quarks and gluons are described as intermetted parton cascades.

[1] K. GEIGER, **SPACE-TIME DESCRIPTION OF ULTRA-RELATIVISTIC NUCLEAR COLLISIONS IN THE QCD PARTON PICTURE**

CERN, TH-Division, CH-121 I Geneva 23, Switzerland, ELSEVIER Physics Reports 258 (1995) 237-376

➤ **Experimental data can provide strong constrains on the models**

Nuclear-nuclear collisions: what are we colliding?

K. Geiger/Physics Reports 258 (1995) 237-376

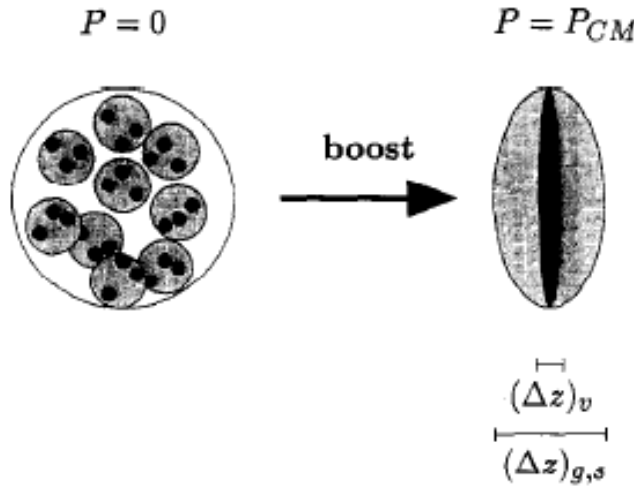
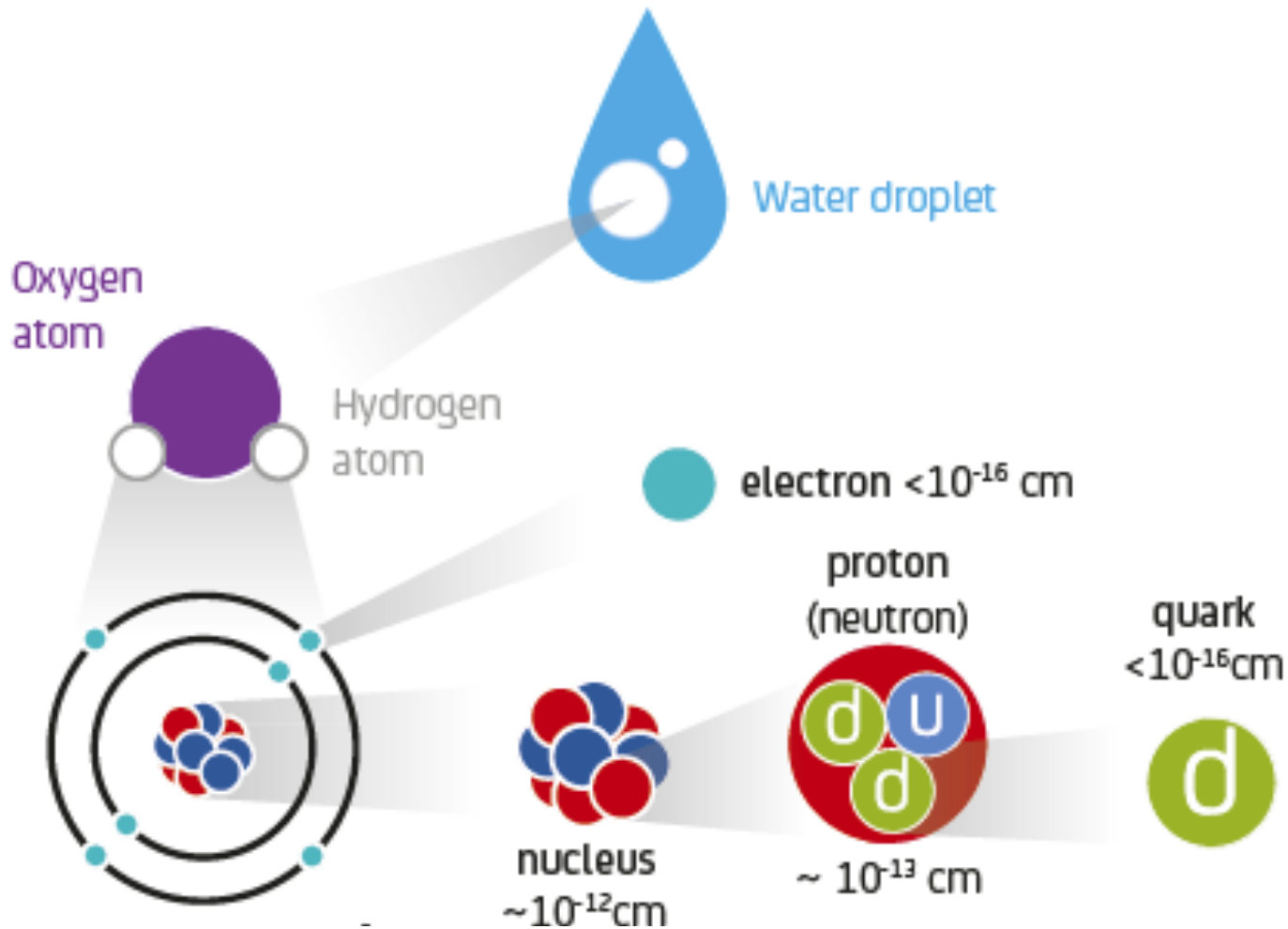


Fig. 19. Distributed Lorentz contraction: The spatial distribution of the partons in the rest frame of each nucleus becomes, after boosting to the *CM* frame, a disc of highly Lorentz contracted valence quarks of $(\Delta z)_v$, surrounded by clouds of softer gluons and sea quarks of $(\Delta z)_{g,s}$.

Микромир



Атом кислорода – 10^{-8} см

"Zoo" of particles:

<http://pdg.lbl.gov>

~ 180 Selected Particles

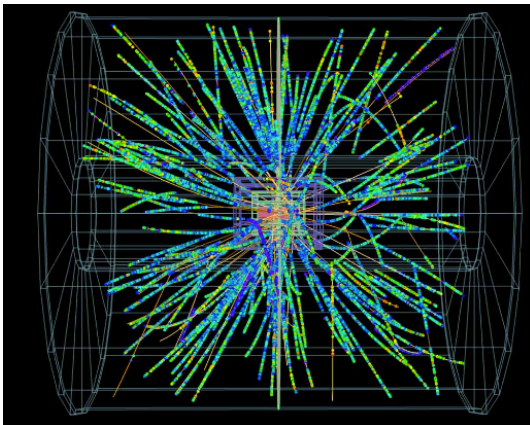
Important Notes:

1. In the detector we see only particles with a sufficiently long lifetime that allows them to be registered:

$\gamma, e, \mu, \pi, K, p, n$

2. To be registered, a particle must experience some interaction with the detector

How to detect particles?



$\pi, W^\pm, Z^0, g, e, \mu, \nu, \nu_e, \nu_\mu, \nu_\tau, \pi^\pm, \pi^0, \eta, f_0(600), g(770),$
 $\omega(782), \eta'(958), f_0(980), a_0(980), \phi(1020), h_1(1170), b_1(1235),$
 $a_1(1260), f_2(1270), f_1(1285), \eta(1295), \pi(1300), a_2(1320),$
 $f_0(1370), f_1(1420), \omega(1420), \eta(1440), a_0(1450), g(1450),$
 $f_0(1500), f_2'(1525), \omega(1650), \omega_3(1670), \pi_2(1670), \phi(1680),$
 $g_3(1690), g(1700), f_0(1710), \pi(1800), \phi_3(1850), f_2(2010),$
 $a_4(2040), f_4(2050), f_2(2300), f_2(2340), K^\pm, K^0, K_S^0, K_L^0, K^*(892),$
 $K_1(1270), K_1(1400), K^*(1410), K_0^*(1430), K_2^*(1430), K^*(1680),$
 $K_2(1770), K_3^*(1780), K_2(1820), K_4^*(2045), D^\pm, D^0, D^*(2007)^0,$
 $D^*(2010)^\pm, D_1(2420)^0, D_2^*(2460)^0, D_2^*(2460)^\pm, D_s^\pm, D_s^{*\pm},$
 $D_{s1}(2536)^\pm, D_{s1}(2573)^\pm, B^\pm, B^0, B^*(5620), B_c^\pm, \eta_c(1S), J/\psi(1S),$
 $\chi_{c0}(1P), \chi_{c1}(1P), \chi_{c2}(1P), \psi(2S), \psi(3770), \psi(4040), \psi(4160),$
 $\psi(4415), \Upsilon(1S), \chi_{b0}(1P), \chi_{b1}(1P), \chi_{b2}(1P), \Upsilon(2S), \chi_{b0}(2P),$
 $\chi_{b2}(2P), \Upsilon(3S), \Upsilon(4S), \Upsilon(10860), \Upsilon(11020), p, n, N(1440),$
 $N(1520), N(1535), N(1650), N(1675), N(1680), N(1700), N(1710),$
 $N(1720), N(2190), N(2220), N(2250), N(2600), \Delta(1232), \Delta(1600),$
 $\Delta(1620), \Delta(1700), \Delta(1905), \Delta(1910), \Delta(1920), \Delta(1930), \Delta(1950),$
 $\Delta(2420), \Lambda, \Lambda(1405), \Lambda(1520), \Lambda(1600), \Lambda(1670), \Lambda(1690),$
 $\Lambda(1800), \Lambda(1810), \Lambda(1820), \Lambda(1830), \Lambda(1890), \Lambda(2100),$
 $\Lambda(2110), \Lambda(2350), \Sigma^+, \Sigma^0, \Sigma^-, \Sigma(1385), \Sigma(1660), \Sigma(1670),$
 $\Sigma(1750), \Sigma(1775), \Sigma(1915), \Sigma(1940), \Sigma(2030), \Sigma(2250), \Xi^0, \Xi^-,$
 $\Xi(1530), \Xi(1690), \Xi(1820), \Xi(1950), \Xi(2030), \Omega^-, \Omega(2250)^-,$
 $\Lambda_c^+, \Lambda_c^0, \Sigma_c(2455), \Sigma_c(2520), \Xi_c^+, \Xi_c^0, \Xi_c^+, \Xi_c^0, \Xi(2645),$
 $\Xi_c(2790), \Xi_c(2815), \Omega_c^0, \Lambda_b^0, \Xi_b^0, \Xi_b^-, t, \bar{t}$

There are many more

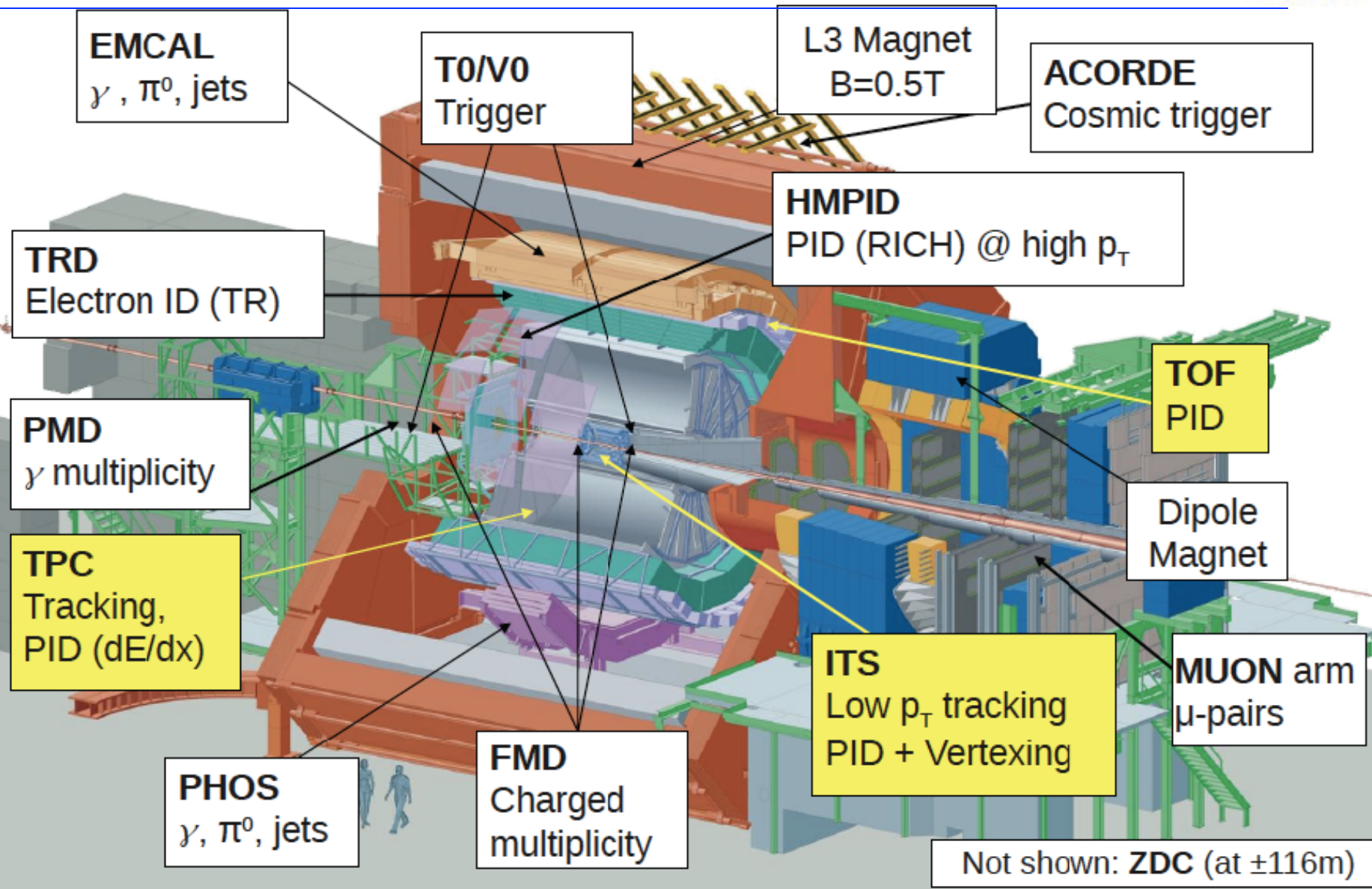
Footprints in the snow



Footprints in the snow



➤ And what are the footprints of different particles?

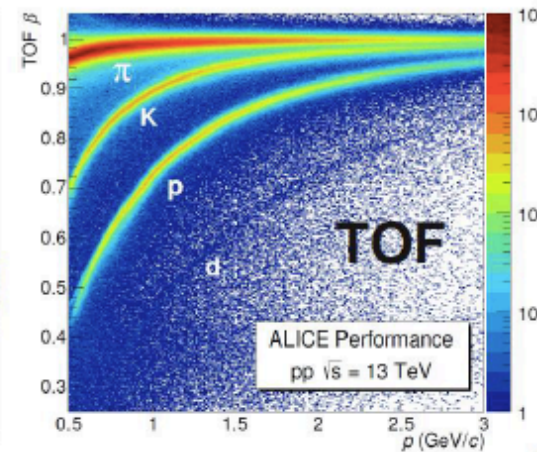
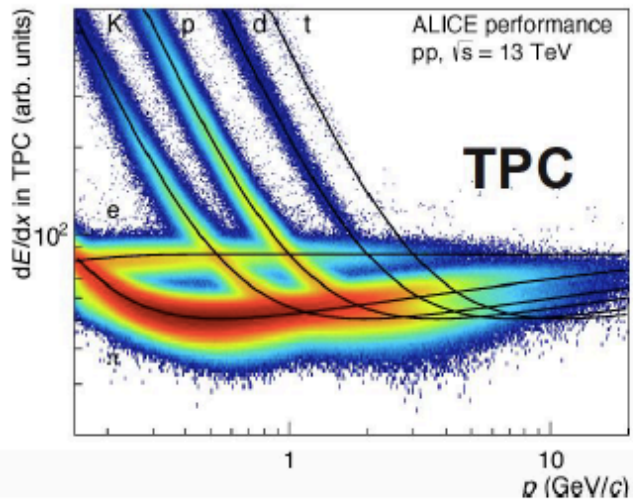
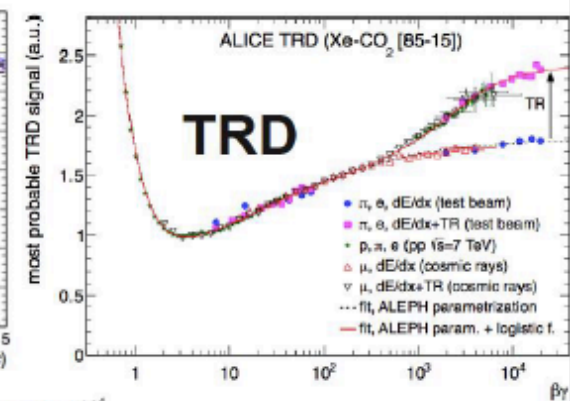
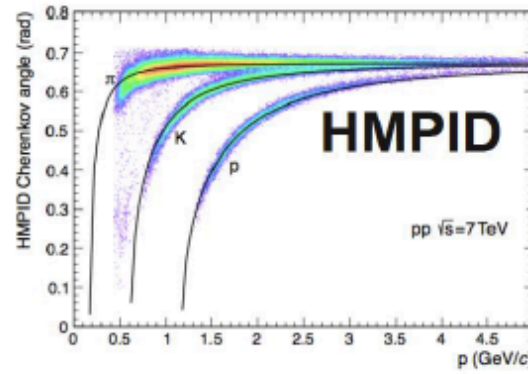
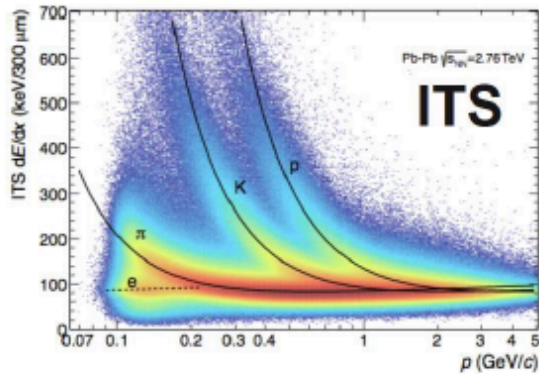


**Nuclear-nuclear collisions:
What do we usually measure?**



Particles tracking and identification

Instrumentation for heavy-ion experiments: PID



→ In order to measure as many different particle species directly, heavy-ion experiments typically have a lot of particle identification (PID) detectors.

[JMP A29 (2014) 1430044]

Observables

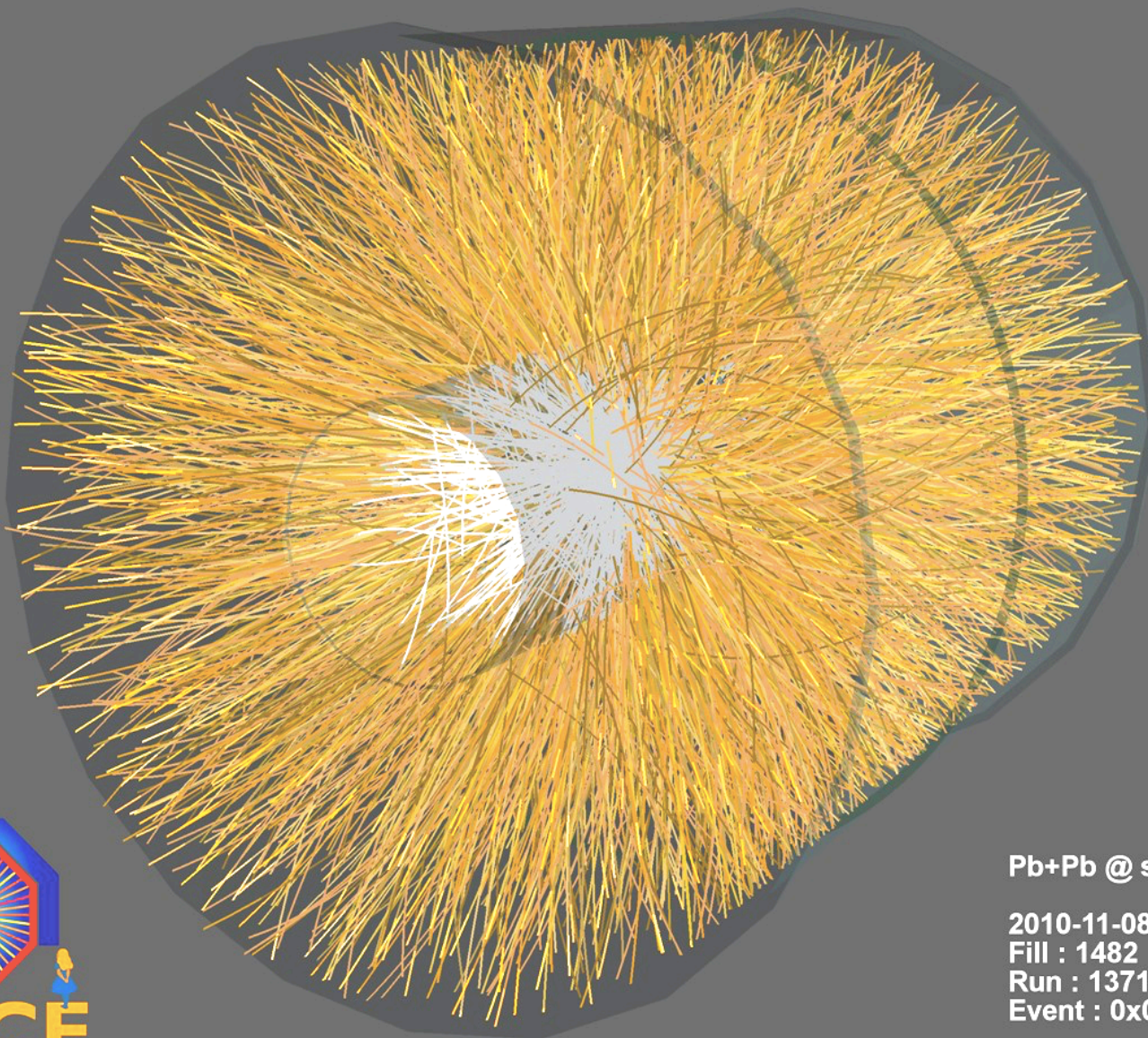
(measured event by event)

- Number of particle tracks, primary and secondary vertices
- Total event charge particle multiplicity (N_{ch})
- Rapidity distribution of charged particles
- Event plane
- Azimuthal flows
- Types of particles and particle ratios (Particle Identification – PID)
- Total event transverse energy (E_{T})

It is important to select the classes of events with similar properties related to the initial conditions

- Centrality determination and different estimators
 - multiplicity classes
 - spectator nucleons (N_{spect}) and number of nucleon-participants (N_{part})

✓ Multiplicity of charged particles in hadronic collisions



Pb+Pb @ $\sqrt{s} = 2.76$ ATeV

2010-11-08 11:30:46

Fill : 1482

Run : 137124

Event : 0x00000000D3BBE693

Nucleus-collisions: what are we observing?

For each particle, you can introduce a **rapidity variable**:

One can also define a rapidity variable:

$$y = \frac{1}{2} \ln \left(\frac{E + p_z c}{E - p_z c} \right).$$

Distribution of particles by rapidity:

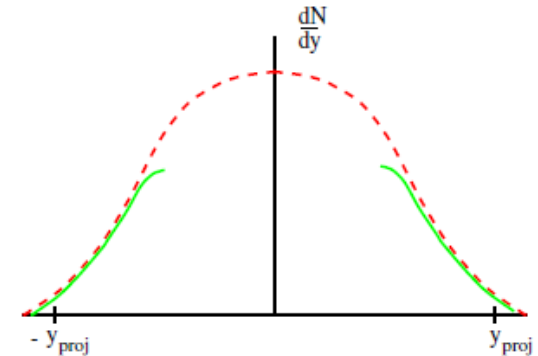
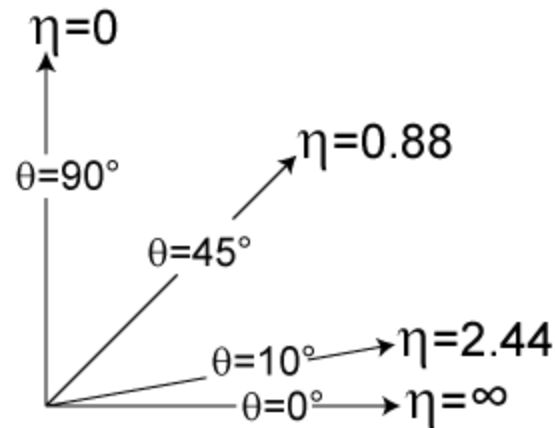


Fig. 18: The rapidity distributions of particles at two different energies

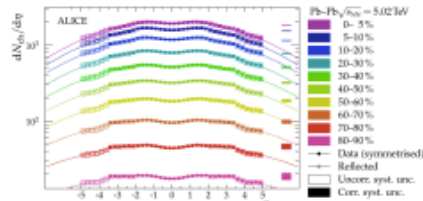
Pseudo-rapidity:

$$\eta = - \ln \left[\operatorname{tg} \left(\frac{\theta}{2} \right) \right],$$



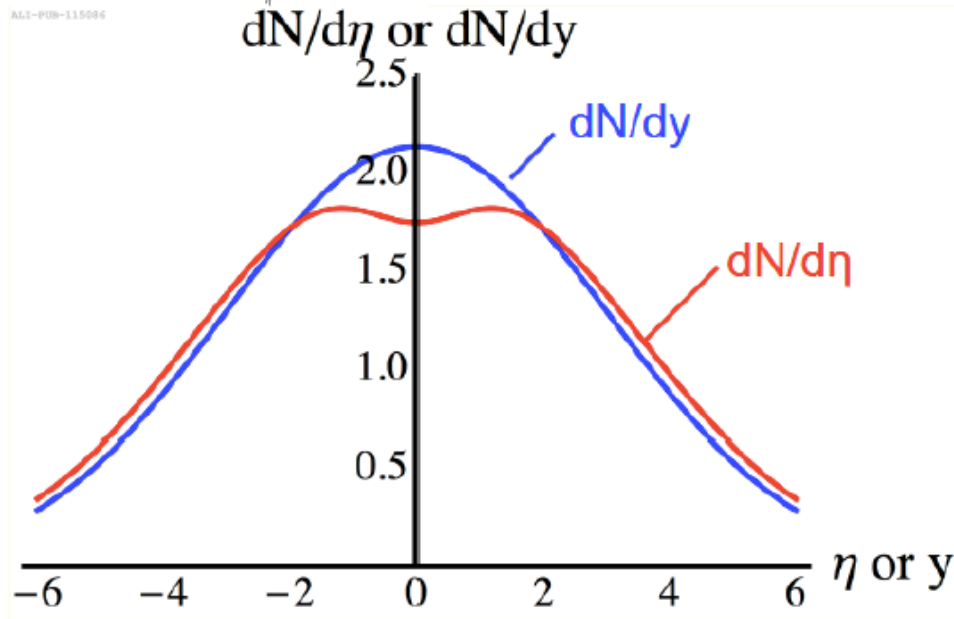
RAPIDITY AND PSEUDORAPIDITY

Short reminder: (Pseudo-)rapidity

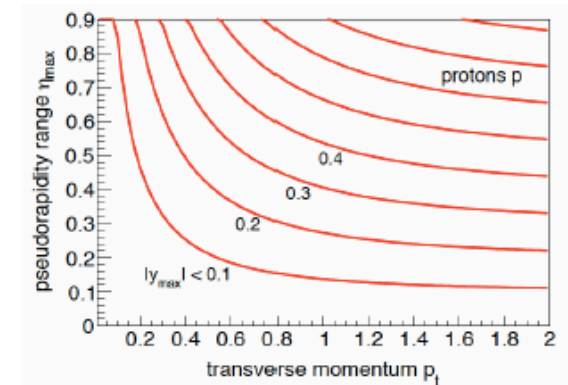


$$\frac{dN}{d\eta} = \sqrt{1 - \frac{m^2}{m_T^2 \cosh^2 y}} \frac{dN}{dy}$$

→ Always keep in mind: Rapidity and pseudo-rapidity are not the same, especially at low transverse momenta!



From: K. Reygers



Alexander.Philipp.Kalweit@cern.ch | CERN-Fermilab school | September 2017 | 10

Nucleus-nucleus collisions: what are we observing?

Pseudorapidity distribution of particle yields in experiments at RHIC:

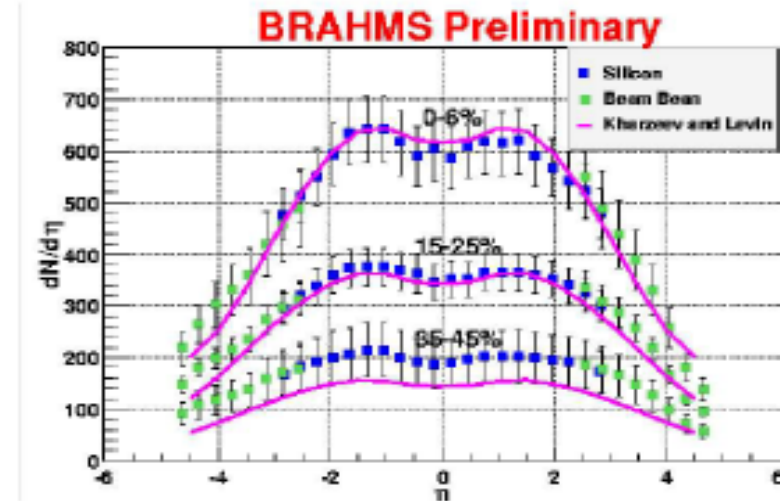
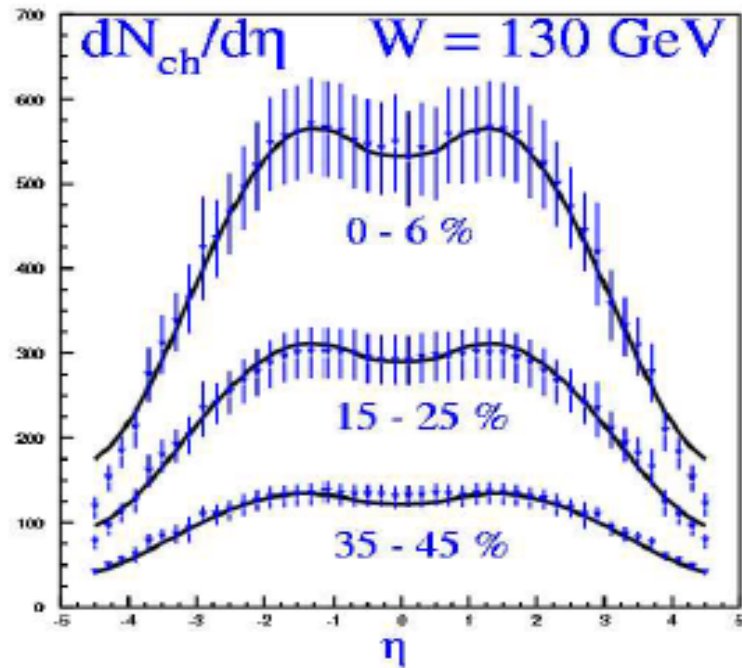


Fig. 28: Colour glass condensate fits to the rapidity density measured in the PHOBOS and BRAHMS experiments

Relativistic heavy-ion physics: three lectures

L. McLerran

Brookhaven National Laboratory, Upton, NY 11973, USA and RIKEN BNL Research Center,
Brookhaven National Laboratory, Upton, NY 11973, USA

Multiplicity distributions in pp collisions

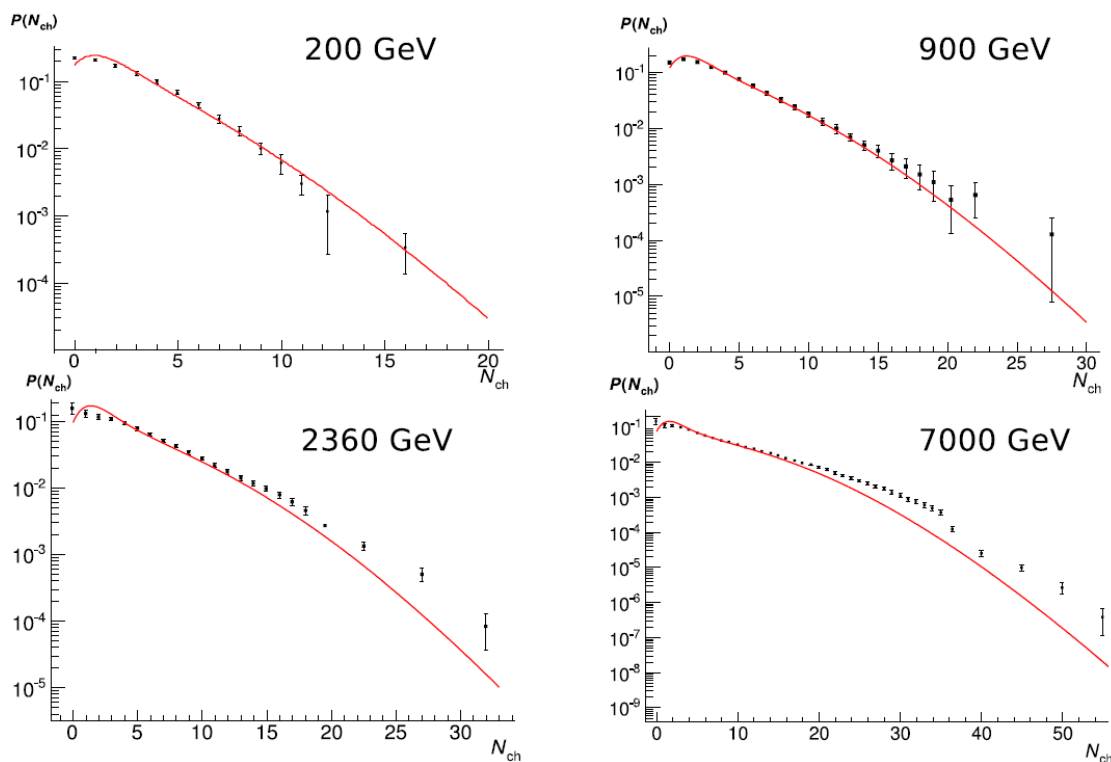


FIGURE 8. Charged particles multiplicity distributions in $p\bar{p}$ collisions at various energies \sqrt{s} (200 GeV, 900 GeV) [25] and in pp collisions (2360 GeV, 7 TeV) [26] in pseudorapidity interval $|\eta| < 0.5$ (dots). The results of the modified multi-pomeron exchange model (lines) are calculated with the model parameters β and t as defined in Fig. 1, 6.

25. V. Khachatryan, et al. (CMS Collaboration), JHEP 1101, 079 (2011).

Model: see E.O.Bodnya*, V.N.Kovalenko†, A.M.Puchkov† and G.A.Feofilov†, “Correlation between mean transverse momentum and multiplicity of charged particles in pp and pp collisions: from ISR to LHC”, PoS, 2013

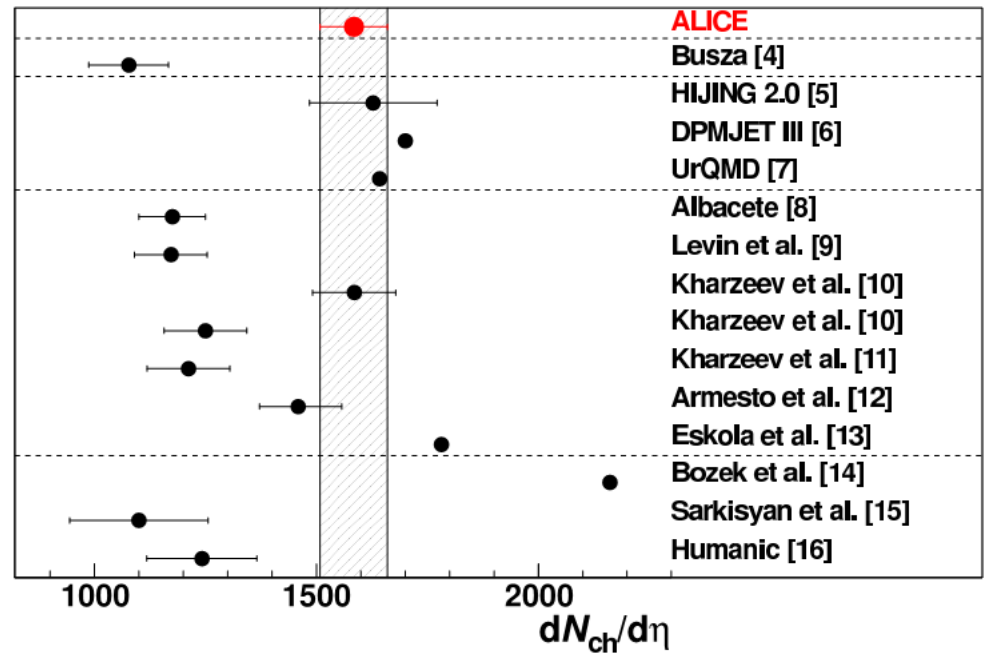
Charged-particle multiplicity density at mid-rapidity

in central Pb-Pb collisions at $\sqrt{s_{NN}} = 2.76$ TeV: :

Multiplicity:

➤ is essential to estimate the initial energy density and it is the 1st important constraint for the models!

$$\varepsilon(\tau) = \frac{E}{V} = \frac{1}{\tau_0 A} \frac{dN}{dy} \langle m_t \rangle$$

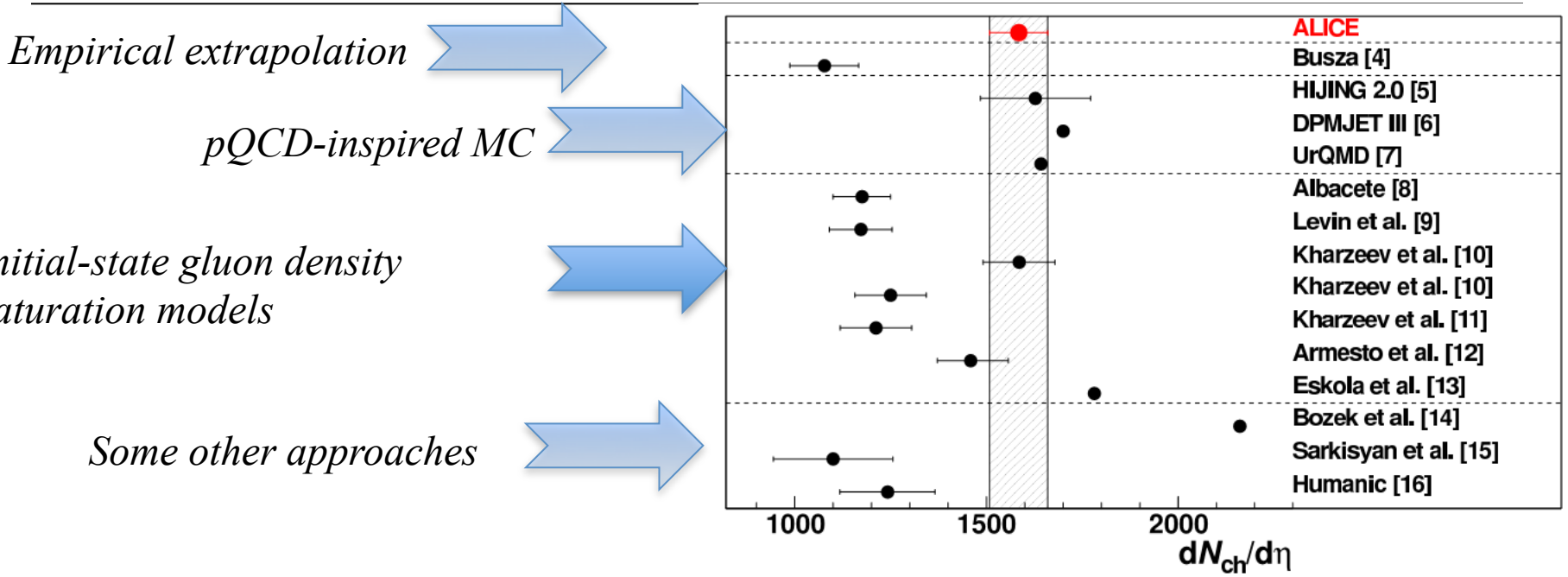


Comparison of ALICE measurement with model predictions.

➤ Bjorken energy density: 2.8 x RHIC for 5% of most central collisions
[arXiv:1011.3916 \[nucl-ex\]](https://arxiv.org/abs/1011.3916), [Phys. Rev. Lett. 105 \(2010\) 252301](https://doi.org/10.1103/PhysRevLett.105.252301)

Charged-particle multiplicity density at mid-rapidity

in central Pb-Pb collisions at $\sqrt{s_{NN}} = 2.76$ TeV: :

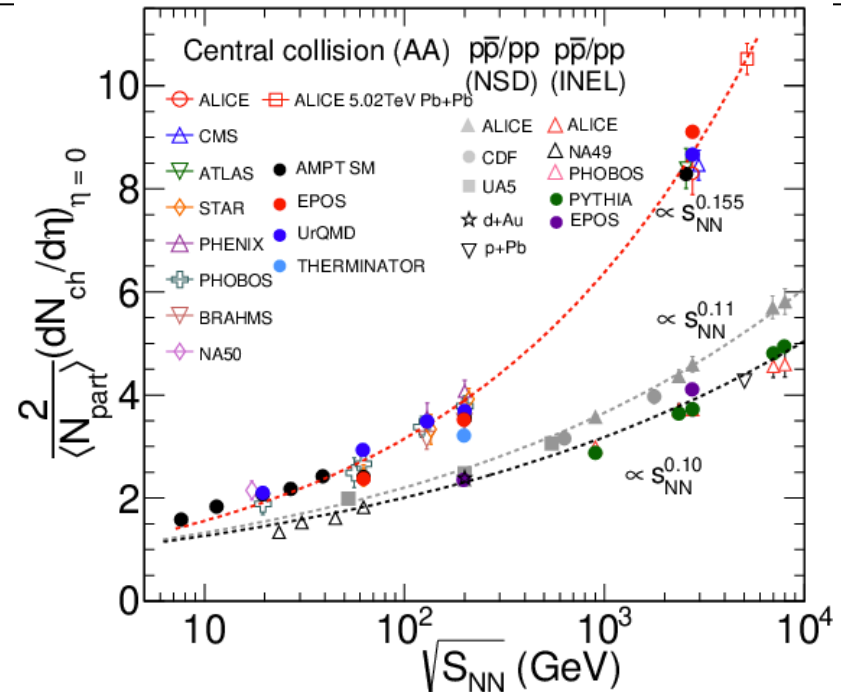


]

ALICE measurement and model predictions

Charged particle pseudo-rapidity density per participant pair for central nucleus-nucleus and non-single diffractive pp (pp) collisions, as a function of $\sqrt{s_{NN}}$

- an increase of about a factor ~ 1.9 relative to pp collisions at similar collision energies,
- an increase of about a factor ~ 2.2 to central Au-Au collisions at $\sqrt{s_{NN}} = 0.2$ TeV !



Basu, Sumit et al - arXiv:2008.07802

- Faster growth with $\sqrt{s_{NN}}$ in AA than in pp!
- Logarithmic extrapolation is ruled out
- Important constraint for the models!

✓ Measurement of p_T of charged particle

Particles tracking and identification

For a particle with charge q ,
moving with speed V in a magnetic field
with intensity B , the Lorentz force acts:

$$F_n = qVB.$$

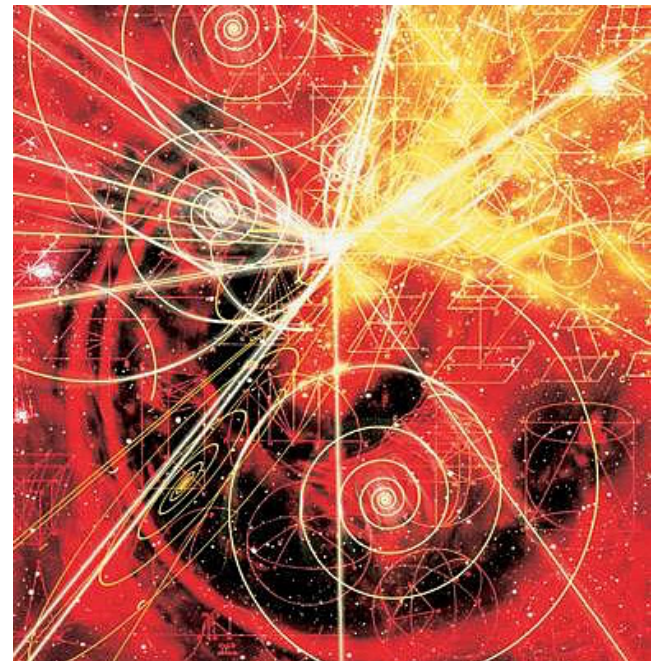
$$qVB = \frac{mV^2}{R}$$

m - particle mass

R – radius of the circle

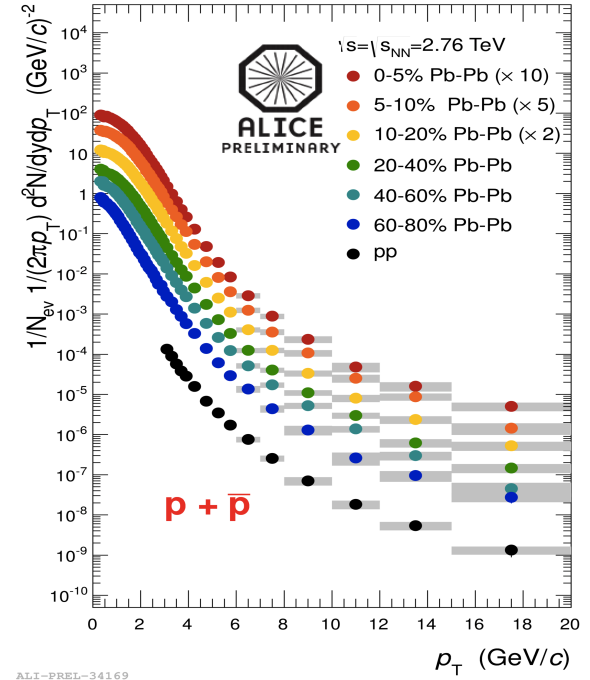
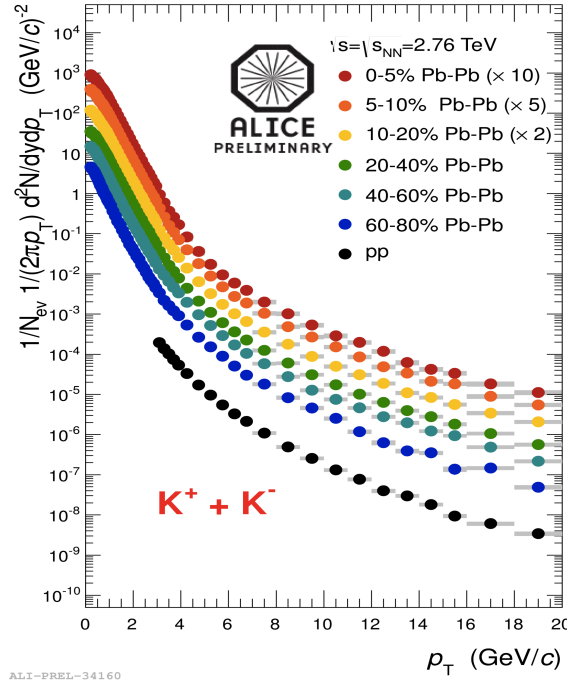
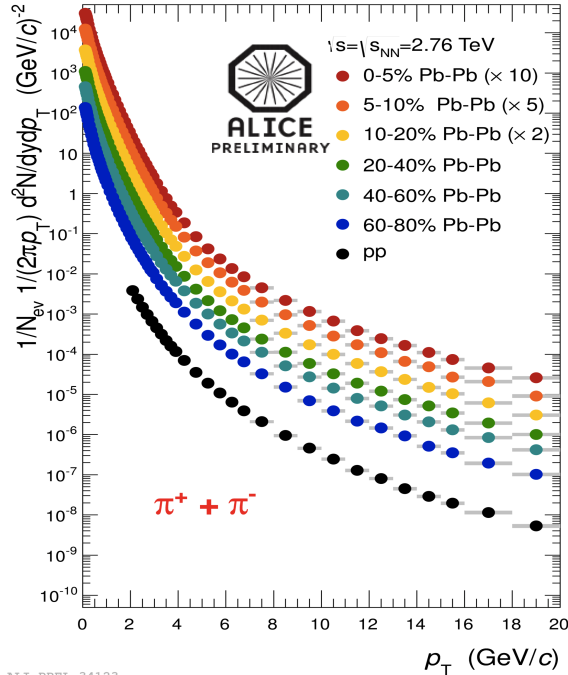
**Having measured R , we will
find the transverse momentum**

$$\mathbf{p}_T = m\mathbf{V}$$



Nucleus-nucleus collisions: what are we observing? Particle distribution by transverse momentum:

Identified-particle p_T spectra up to 20 GeV/c



95 % of all particles below 1.5 GeV/c : particle production non-perturbative process

- **Low- $p_T < 2$ GeV/c** : dynamics of bulk matter described by **Relativistic Hydrodynamic Models (RHD)**
- **High- $p_T > 8$ GeV/c** : spectra reflect interaction of partons from hard scatterings with the medium
- **Intermediate p_T $2 < p_T < 8$ GeV/c** : interplay of soft and hard processes

✓ Transverse energy in the event

Transverse energy of charged particles and Bjorken energy density

S_{\perp} – is the transverse overlap area of the colliding nuclei

$$\epsilon \cdot \tau = \frac{dE_{\perp}}{dy} \frac{1}{S_{\perp}}$$

E_{\perp} – is the total transverse energy

τ – is the formation time

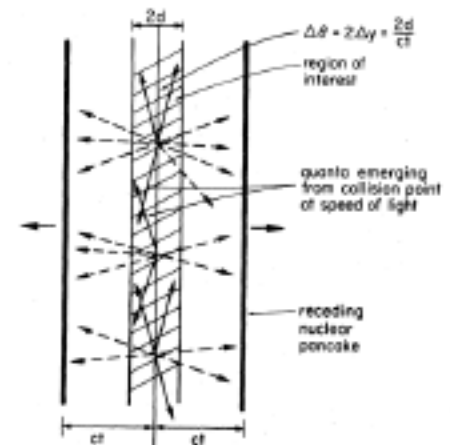
$$\tau \sim 1 \text{ fm}/c$$

$$\frac{d\langle E_{\perp} \rangle}{dy} \approx \frac{3}{2} \left(\langle m_{\perp} \rangle \frac{dN}{dy} \right)_{\pi^{\pm}} + 2 \left(\langle m_{\perp} \rangle \frac{dN}{dy} \right)_{K^{\pm}, p, \bar{p}} \quad [2]$$

The factors 3/2 and 2 compensate for the neutral particles.

$$\epsilon = \frac{dE_{\perp}}{dy} \frac{1}{S_{\perp} \cdot \tau} \quad [1]$$

$$\langle m_{\perp} \rangle = \sqrt{\langle p_{\perp} \rangle^2 + m^2}$$



$$\epsilon \approx 1 \text{ GeV}/\text{fm}^3$$

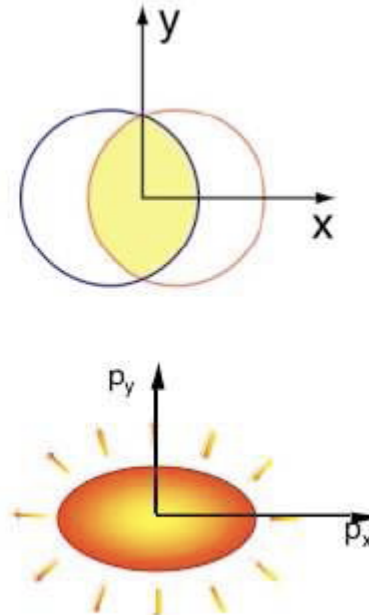
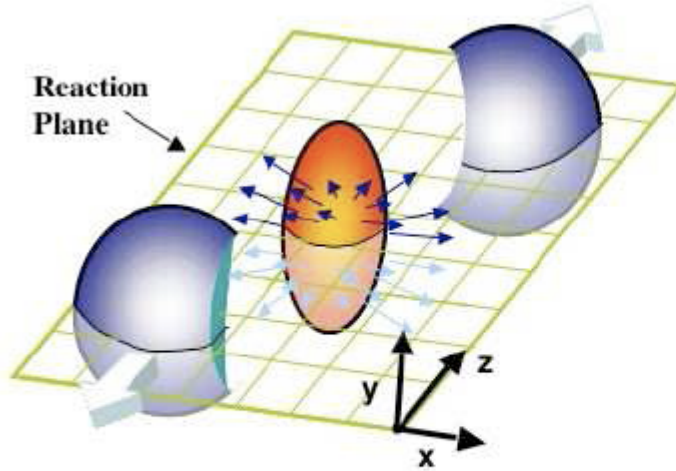
is critical energy density

[1] J. D. Bjorken, Phys. Rev. D 27, 140 (1983)

[2] B. I. Abelev, M. M. Aggarwal et al.

✓ Reaction and Event planes in AA collisions

Эллиптический поток в Pb-Pb столкновениях при энергии $\sqrt{s_{NN}} = 2.76$ TeV:



Tannebaum' 06

$$E \frac{d^3 N}{d^3 p} = \frac{1}{2\pi} \frac{d^2 N}{p_t dp_t dy} \left(1 + \sum_{n=1}^{\infty} 2v_n \cos[n(\phi - \Psi_R)] \right)$$

$$v_2 = \langle \cos 2(\phi - \Psi_R) \rangle = \left\langle \frac{p_x^2 - p_y^2}{p_T^2} \right\rangle$$

Excintricity: $\epsilon_x = \frac{\langle y^2 - x^2 \rangle}{\langle y^2 + x^2 \rangle}$

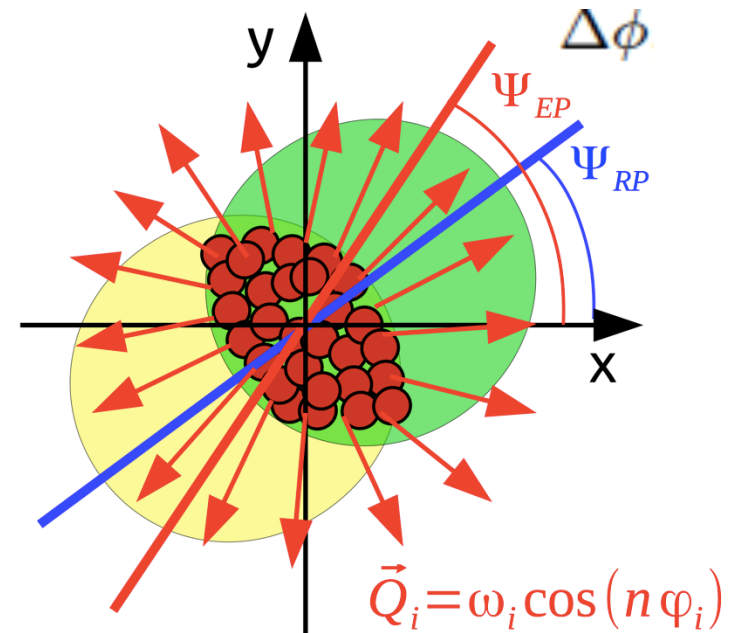
2- and 4-particle cumulant methods: $v_2\{2\}$ and $v_2\{4\}$

Reaction Plane (RP) and Event plane (EP) [1]

- **Reaction plane (RP)** –the plane formed by the impact parameter b and the beam line

RP cannot be measured in the experiment since we cannot measure b

- **Event plane (EP)** is the observable estimation of the reaction plane



[1] Jean-Yves Ollitrault, Reconstructing azimuthal distributions in nucleus–nucleus collisions, arXiv:nucl-ex/9711003v2

Reaction Plane (RP) and Event plane (EP) [1]

The following relation between measured and true Fourier coefficients[1]:

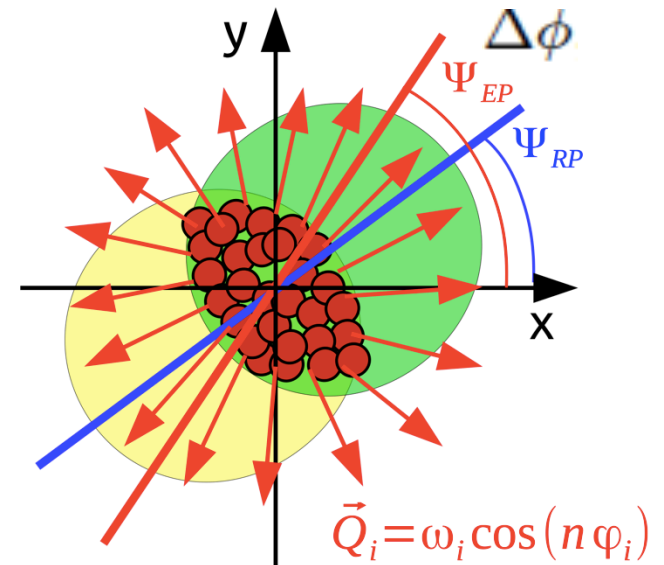
$$\langle \cos n\psi \rangle = \langle \cos n\phi \rangle \langle \cos n\Delta\phi \rangle.$$

, the vector obtained by summing all the transverse momenta of the particles produced in the projectile (target) rapidity region is parallel (antiparallel) to the impact parameter. One constructs a vector \mathbf{Q} :

$$\mathbf{Q} = \sum_{k=1}^N w_k \mathbf{u}_k$$

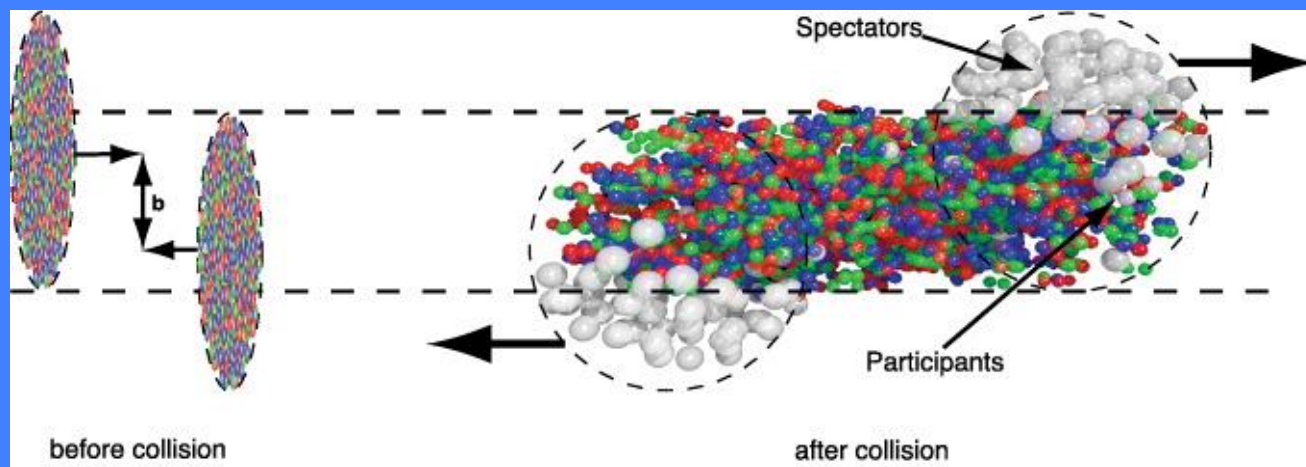
where the sum runs over all the detector particles in the event, w_k – weight, \mathbf{u}_k – is a unit vector parallel to transverse momentum of the particle

\mathbf{Q} – lies in the true reaction plane and azimuthal distributions can be measured from \mathbf{Q}

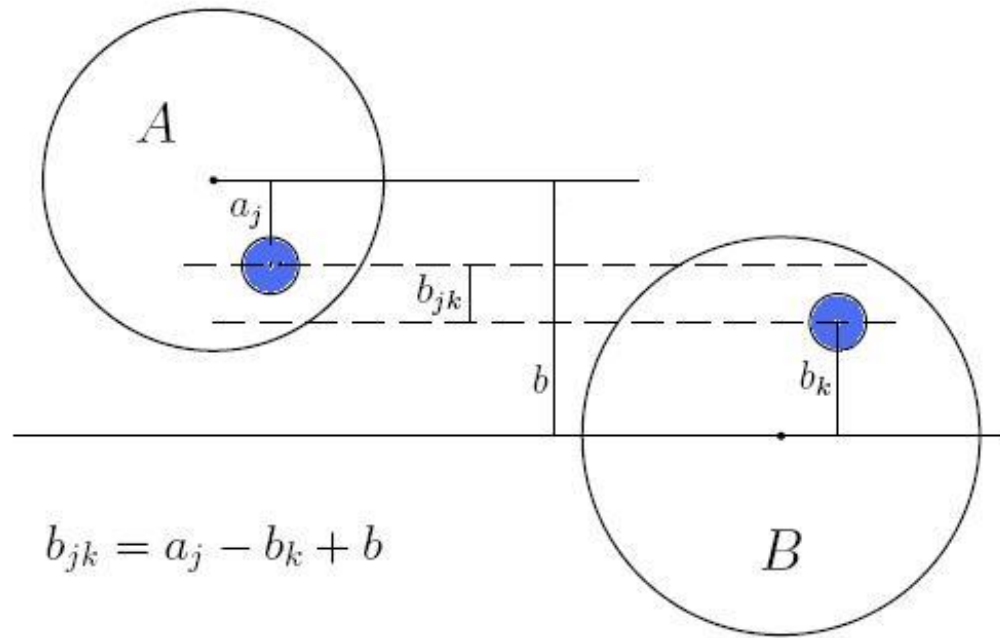


[1] Jean-Yves Ollitrault, Reconstructing azimuthal distributions in nucleus–nucleus collisions, arXiv:nucl-ex/9711003v2

✓ Selection of central events in AA collisions



Centrality of collisions



$$b_{jk} = a_j - b_k + b$$

Nucleons —

participants and spectators

$$N_{\text{spec}} = 2A - N_{\text{part}}$$

Binary collisions — N coll

$$\rho(r) = \rho_0 \left\{ 1 + \exp\left(\frac{r-R_A}{a}\right) \right\}^{-1} \quad \text{or} \quad \rho(r) = \rho_0 \frac{1 + w(r/R)^2}{1 + \exp\left(\frac{r-R}{a}\right)}$$

$$R_A = R_0 \cdot A^{1/3}$$

$$R_0 = 1.07 \text{ fm,}$$

$$a = 0.545 \text{ fm}$$

The parameters are based on data from low-energy electron-nucleus scattering experiments [22].

[22] H. De Vries, C. W. De Jager, and C. De Vries, *At. Data Nucl. Data Tables* **36**, 495 (1987).

$$\int \rho(r) d^3r = A$$

We require a hard-sphere exclusion distance of $d_{\text{min}} = 0.4 \text{ fm}$ between the centers of the nucleons, i.e., no pair of nucleons inside

the nucleus has a distance less than d_{min} . 41

The centrality percentile c of A-A collision with an impact parameter b

$$c = \frac{\int_0^b d\sigma/db' db'}{\int_0^\infty d\sigma/db' db'} = \frac{1}{\sigma_{AA}} \int_0^b \frac{d\sigma}{db'} db'. \quad (1)$$

$$c \approx \frac{1}{\sigma_{AA}} \int_{N_{\text{ch}}^{\text{THR}}}^\infty \frac{d\sigma}{dN'_{\text{ch}}} dN'_{\text{ch}} \approx \frac{1}{\sigma_{AA}} \int_0^{E_{\text{ZDC}}^{\text{THR}}} \frac{d\sigma}{dE'_{\text{ZDC}}} dE'_{\text{ZDC}}. \quad (2)$$

db

Centrality of relativistic heavy ion collisions

In various experiments:

ALICE as an example

PHYSICAL REVIEW C **88**, 044909 (2013)

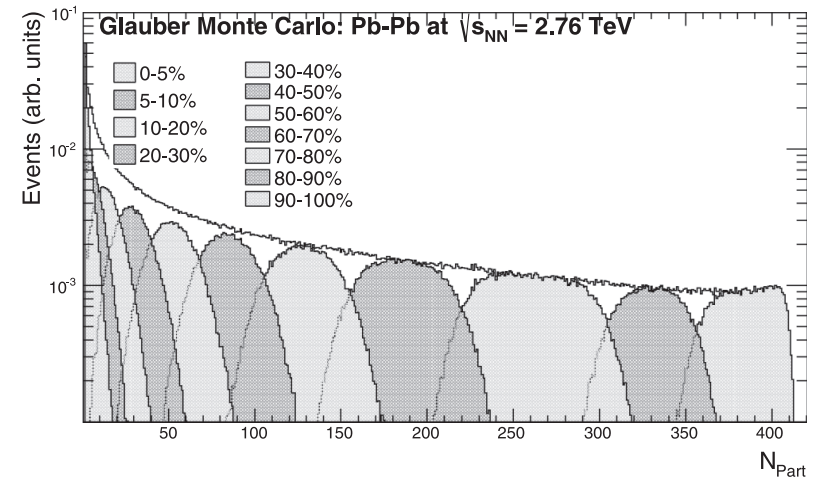
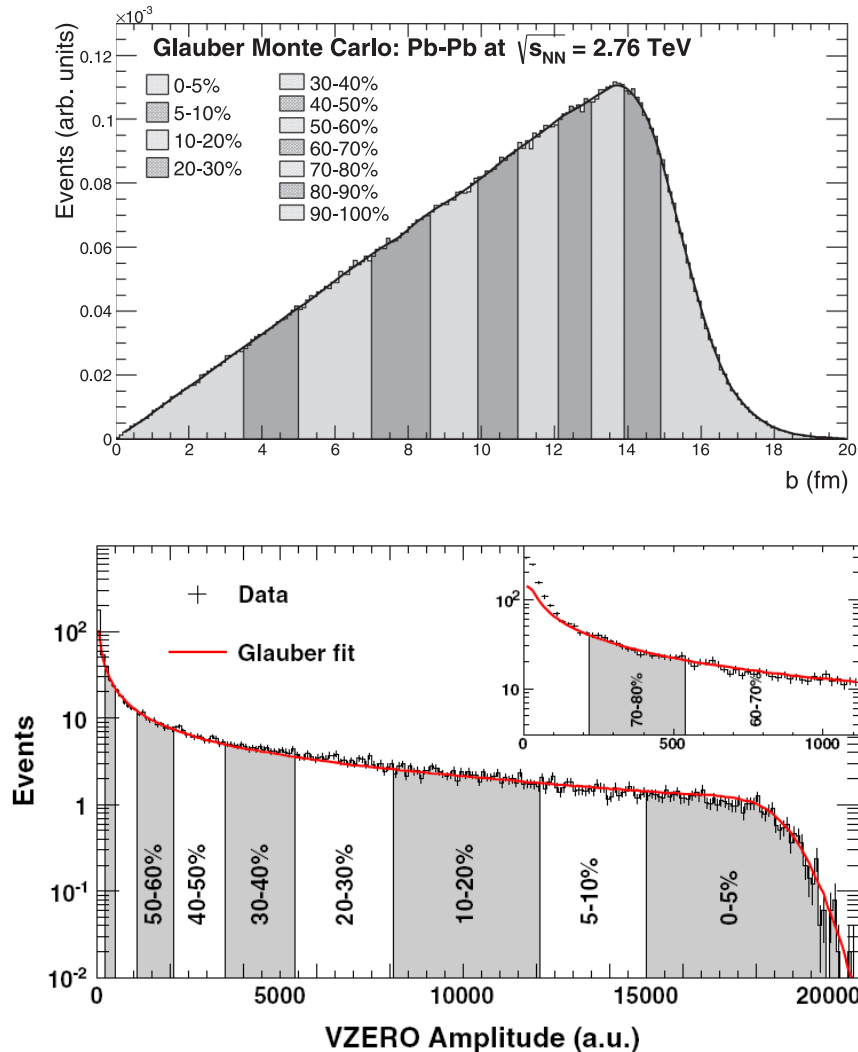
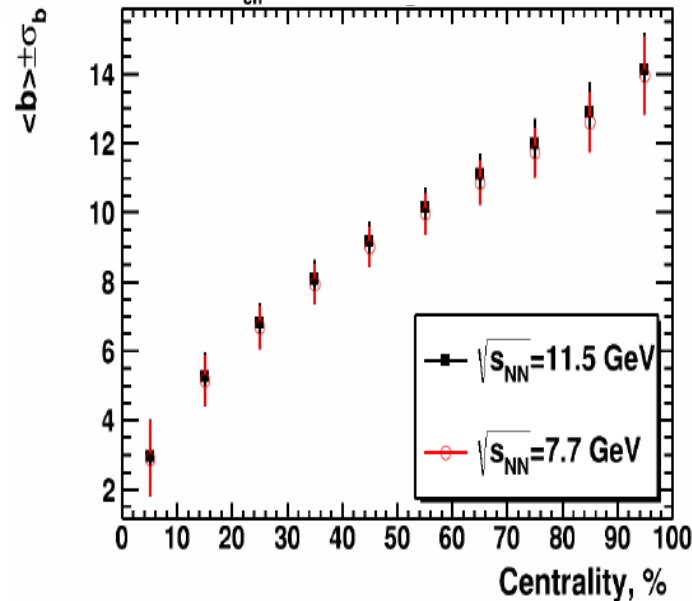
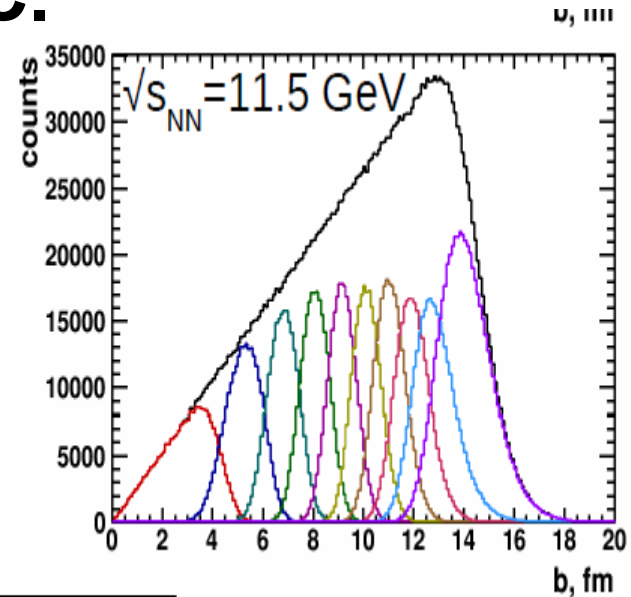
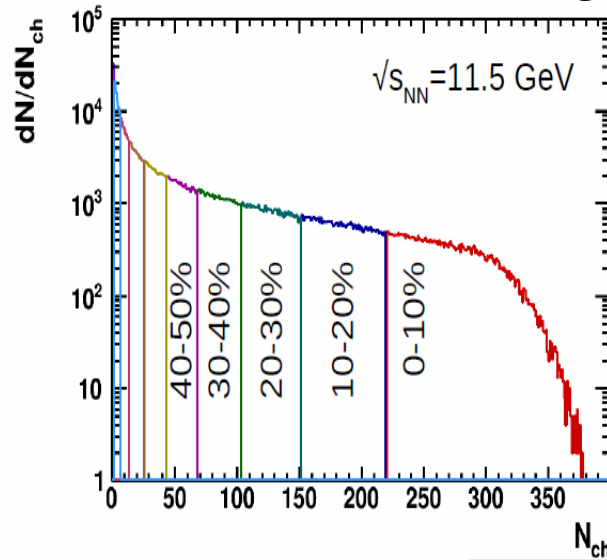


FIG. 10. (Color online) Distribution of the sum of amplitudes in the VZERO scintillators. The distribution is fitted with the NBD-Glauber fit (explained in the text), shown as a line. The centrality classes used in the analysis are indicated in the figure. The inset shows a zoom of the most peripheral region.

Example: Centrality determination with multiplicity in TPC.



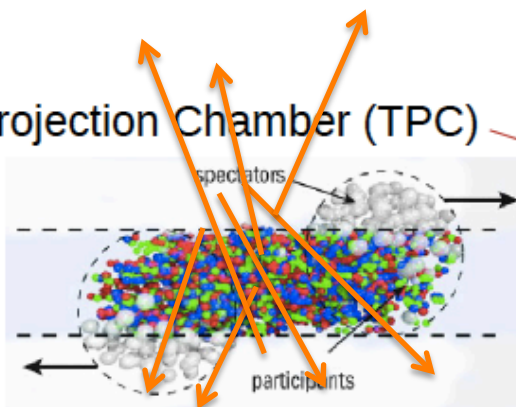
Report by Alexander Ivashkin, Petr Parfenov, Classes of centrality for the 1st MPD data analysis data, PWG1 meeting, 16.01.2020

Two main approaches to centrality classes selection at MPD:

1) Charged particle Multiplicity classes by the TPC (or...) and

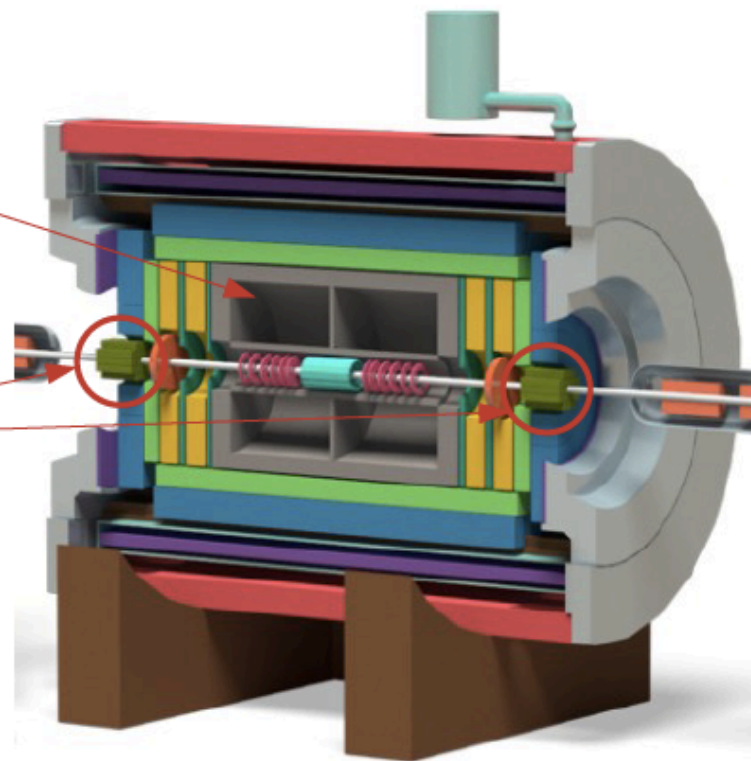
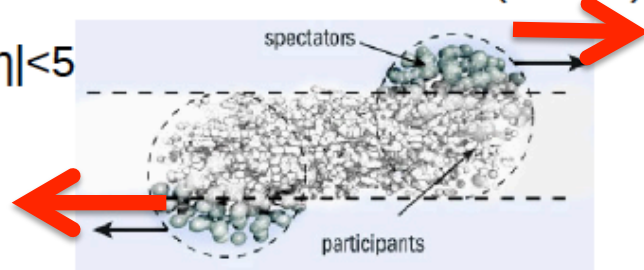
- Time Projection Chamber (TPC)

$$|\eta| < 1.5$$



- Forward Hadron Calorimeter (FHCaI)

$$2 < |\eta| < 5$$



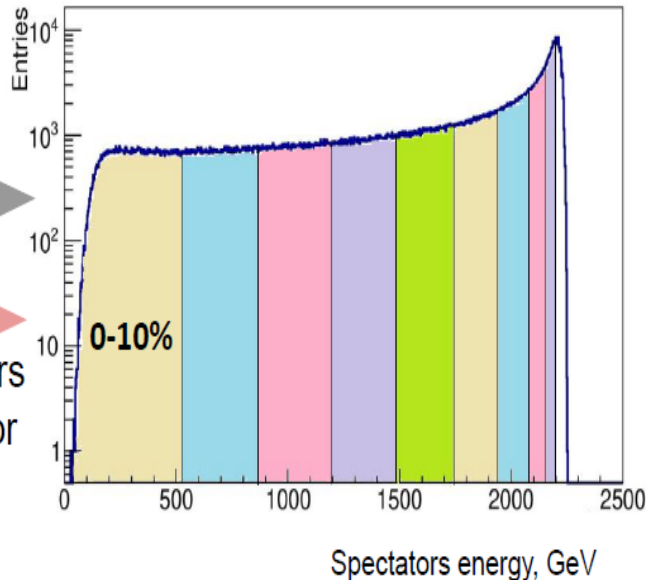
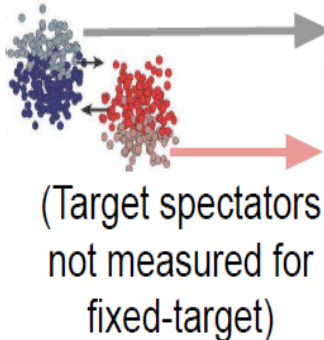
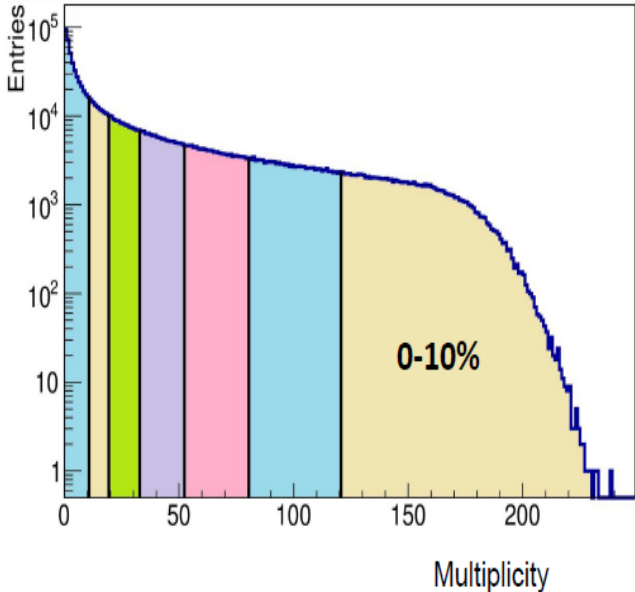
2) Spectator energy classes by FHCaI

Centrality estimations

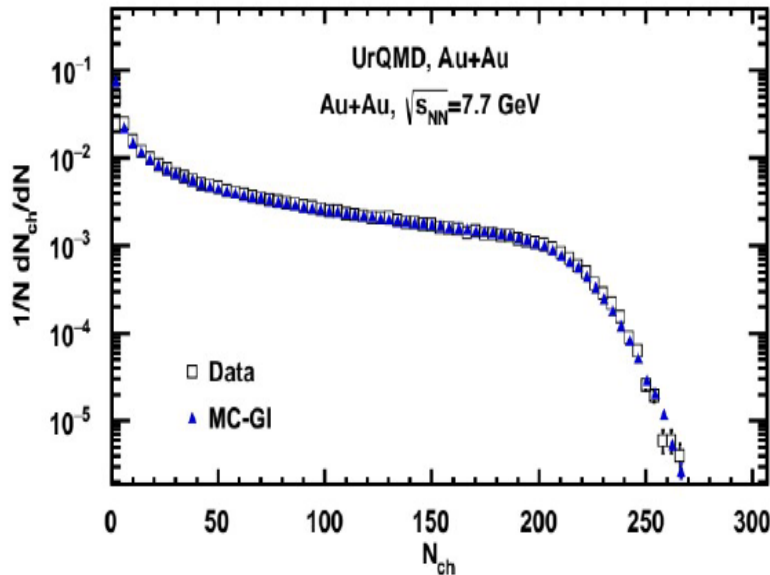
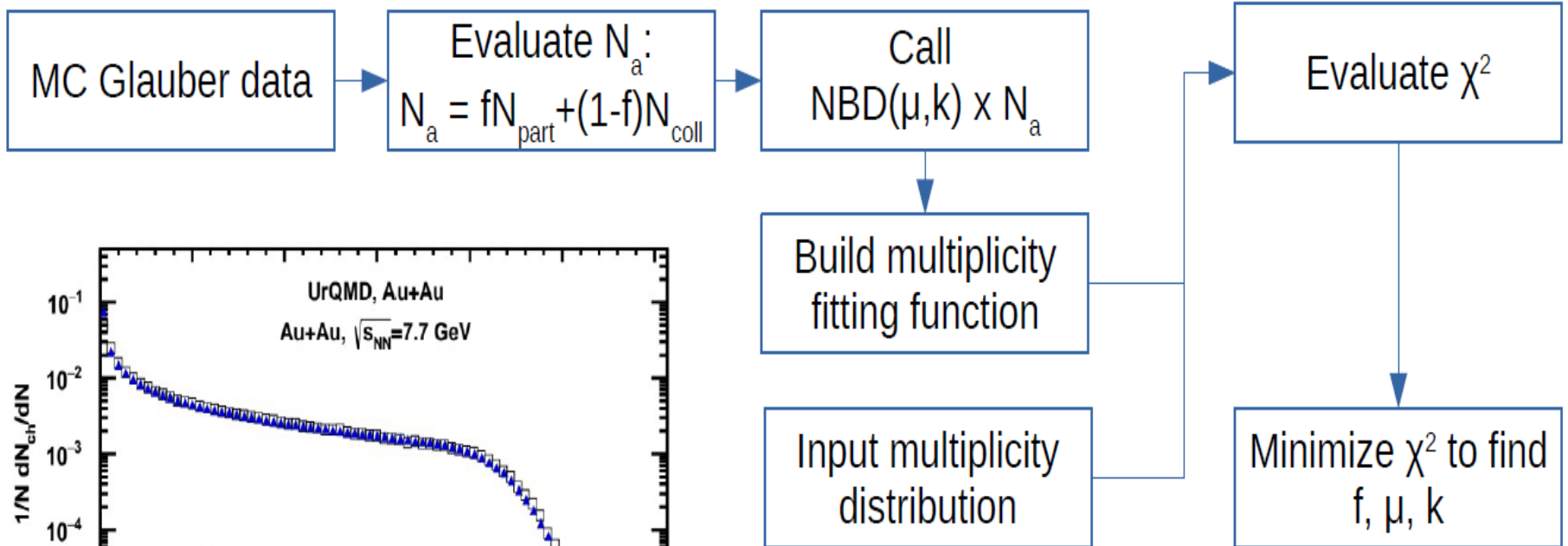
Types of centrality estimators

Produced charged particles

Spectators



Centrality from TPC multiplicity: usual procedure



NBD – negative binomial distribution

Parameters of the fit:

- **f** – fraction of the production from the soft component
- **μ** – mean multiplicity value
- **k** – width of the multiplicity distribution, can be connected to the fluctuations

Glauber model assumptions:

MC Glauber model provides a description of the initial state of a heavy-ion collision

- Independent straight line trajectories of the nucleons
- A-A collision is treated as a sequence of independent binary NN collisions
- Monte-Carlo sampling of nucleons position for individual collisions

Main model parameters

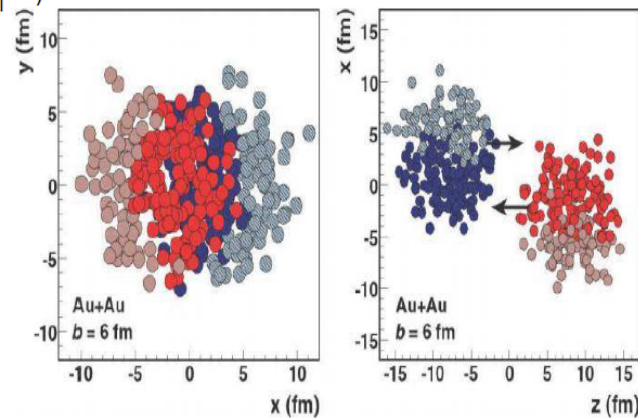
- Colliding nuclei
 - Inelastic nucleon-nucleon cross section ($\sigma_{\text{inel}}^{\text{NN}}$) (depends on collision energy)
 - Nuclear charge densities (Wood-Saxon distribution)

$$\rho(r) = \rho_0 \cdot \frac{1 + w(r/R)^2}{1 + \exp\left(\frac{r-R}{a}\right)}$$

Geometry parameters

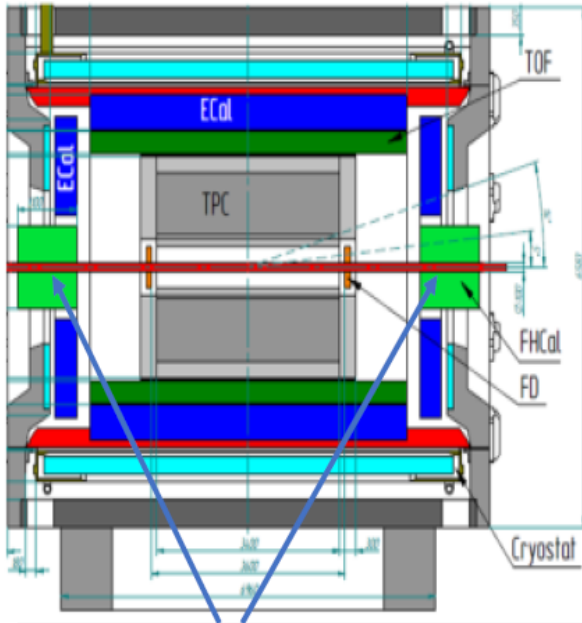
- b – impact parameter
- N_{part} – number of nucleons participating in the collision
- N_{spec} – number of spectator nucleons in the collision
- N_{coll} – number of binary NN collisions

Glauber Modeling in High Energy Nuclear Collisions:
ARNPS57:205-243,2007

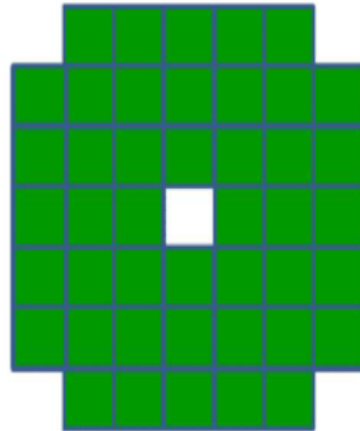


➤ **NB! These assumptions can produce a noticeable bias in N_{coll} and in R_{AA} (!)**
see [1] G.Feofilov et al, PEPAN, 52, № 4, 2021, 584-590,
<https://link.springer.com/article/10.1134/S1063779621040043>

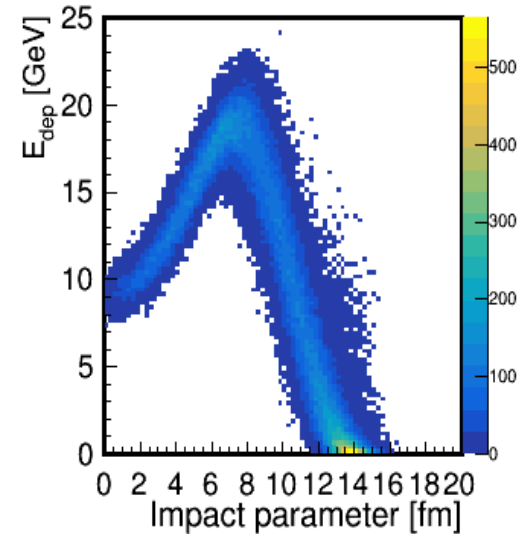
FHCal for centrality



Two upstream/downstream parts

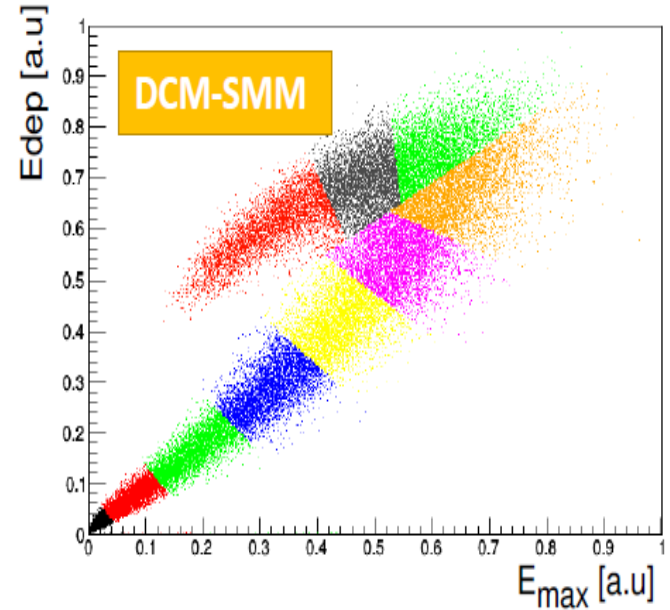
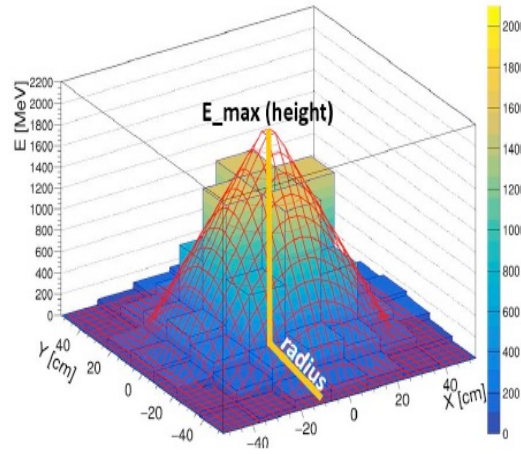
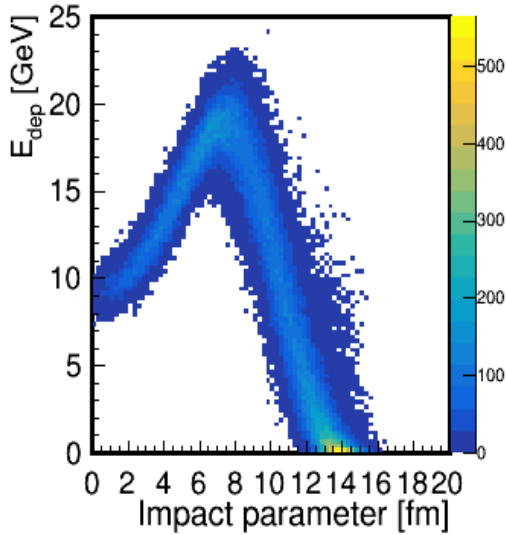


FHCal modules



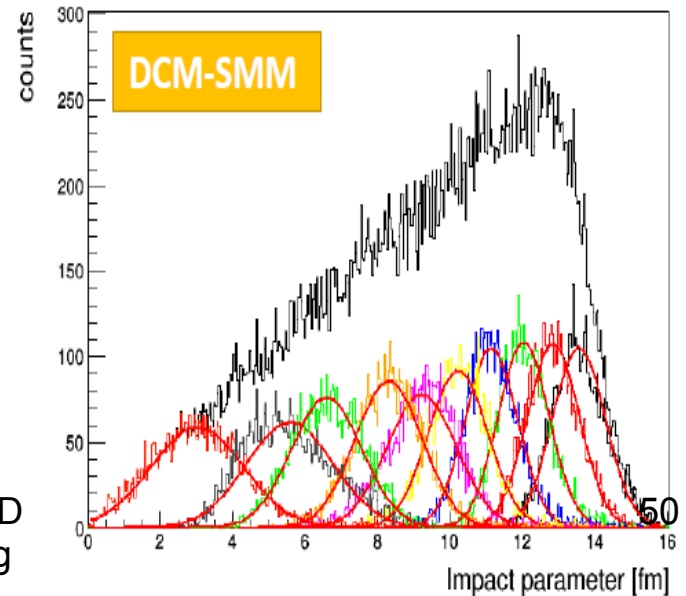
Due to the central hole in FHCal for the beam pipe some spectators can escape detection which will lead to the horn shape in the total deposited energy distribution

FHCAL for centrality



The main smearing factor in the spectator energy deposit estimator for the centrality would be the spectators which escaped detection.

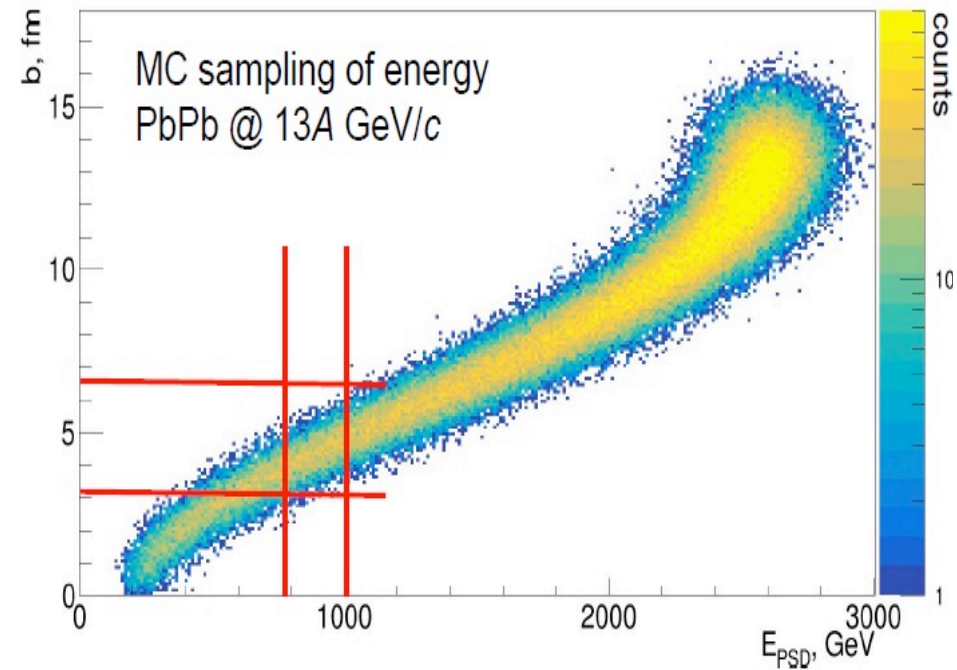
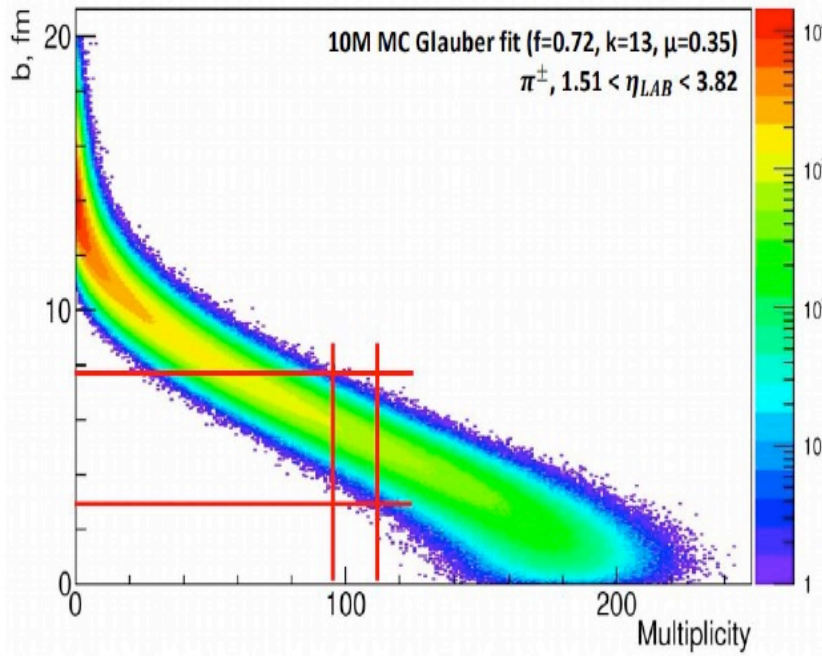
This leads to the possibility of mismatching centrality classes from very central with very peripheral events



Centrality estimations vs. impact parameter

Centrality estimators based on charged track multiplicity in TPC and spectator energy deposit in FHCaI both give only a rather wide estimation of actual impact parameter of the collision

It can be worth it to have a method of combined estimation of the centrality to reduce these fluctuations of the centrality vs. impact parameter



Problems:

Centrality and widths of centrality class in relativistic heavy ion collisions

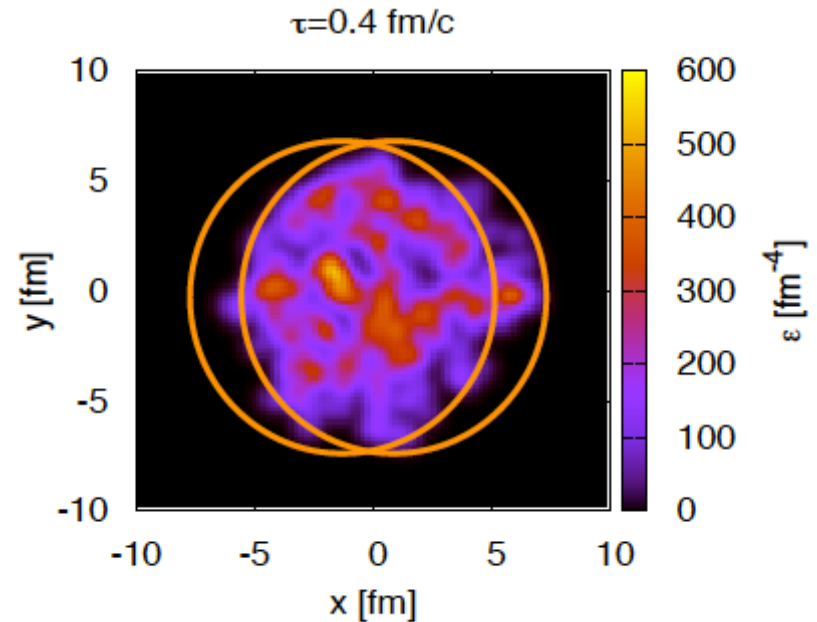
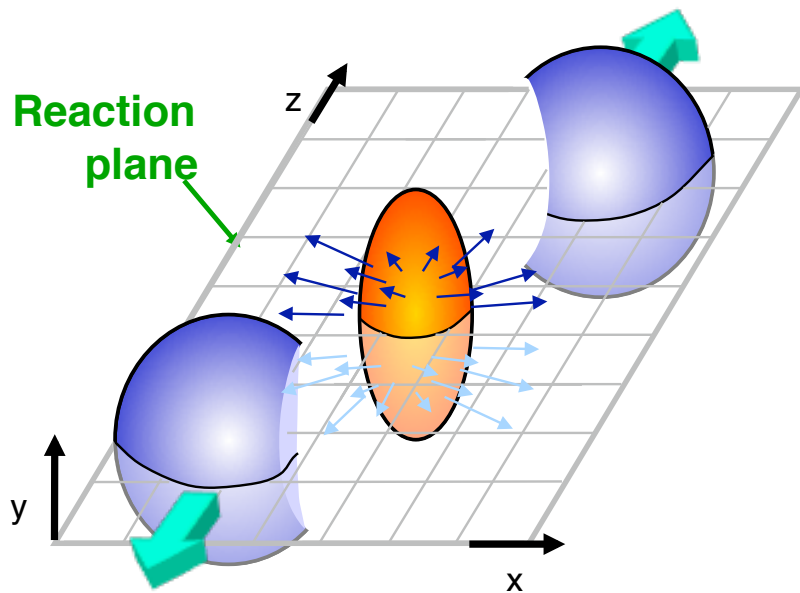


Figure 3. Geometry of a non-central heavy ion collision (left panel). Density fluctuations in the transverse plane in a sample collision event (right panel).

Berndt Müller, Arxiv 1309.7612v2 12 Oct2013

- Density fluctuations in any single event and trivial volume fluctuations could be mixed in case of the wide width of centrality class

Centrality class width

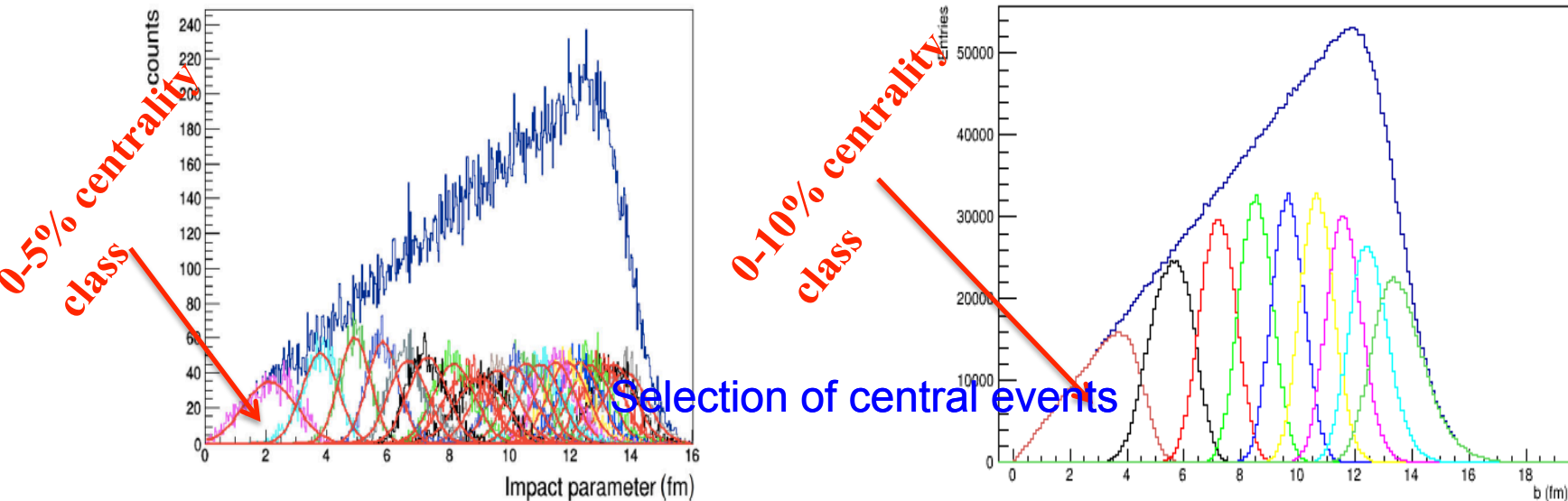


Fig. 44 Top: correlation of the energy deposition in the FHCAL and the height of the cone, obtained from the linear fit of the two two-dimensional energy distributions in the FHCAL modules. The different colors indicate groups of events within 5% centrality ranges. Bottom: distributions of the MC-generated impact parameters for each 5% group of events fitted to a Gaussian

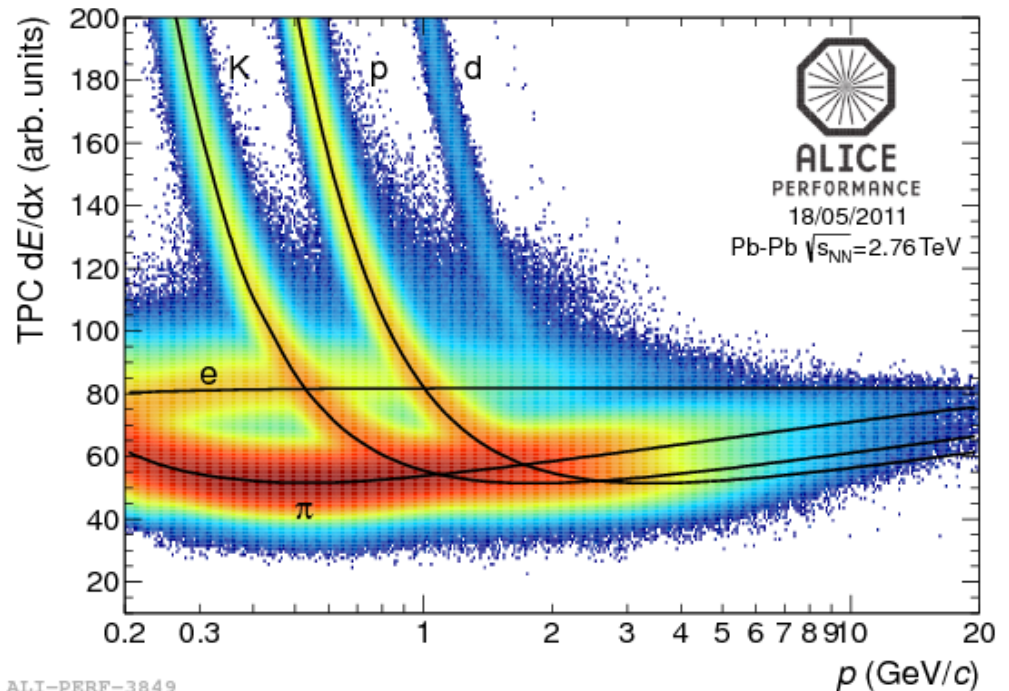
- we need **more precise** selection of centrality classes
- we need events with well **defined initial conditions** and optimized class width
- we need combination of **several observables** – proxies of centrality, capable to minimize trivial volume fluctuations

✓ **A short addition: one important application in medicine**

In addition: ionization losses and applications in hadron therapy of oncology disease

Bethe-Bloch formula:
Energy loss dE for ionization of atoms after passing through a layer of thickness dx by the particle with charge Z_{eff} flying with speed β in a medium with electron density n_e and average ionization energy I .

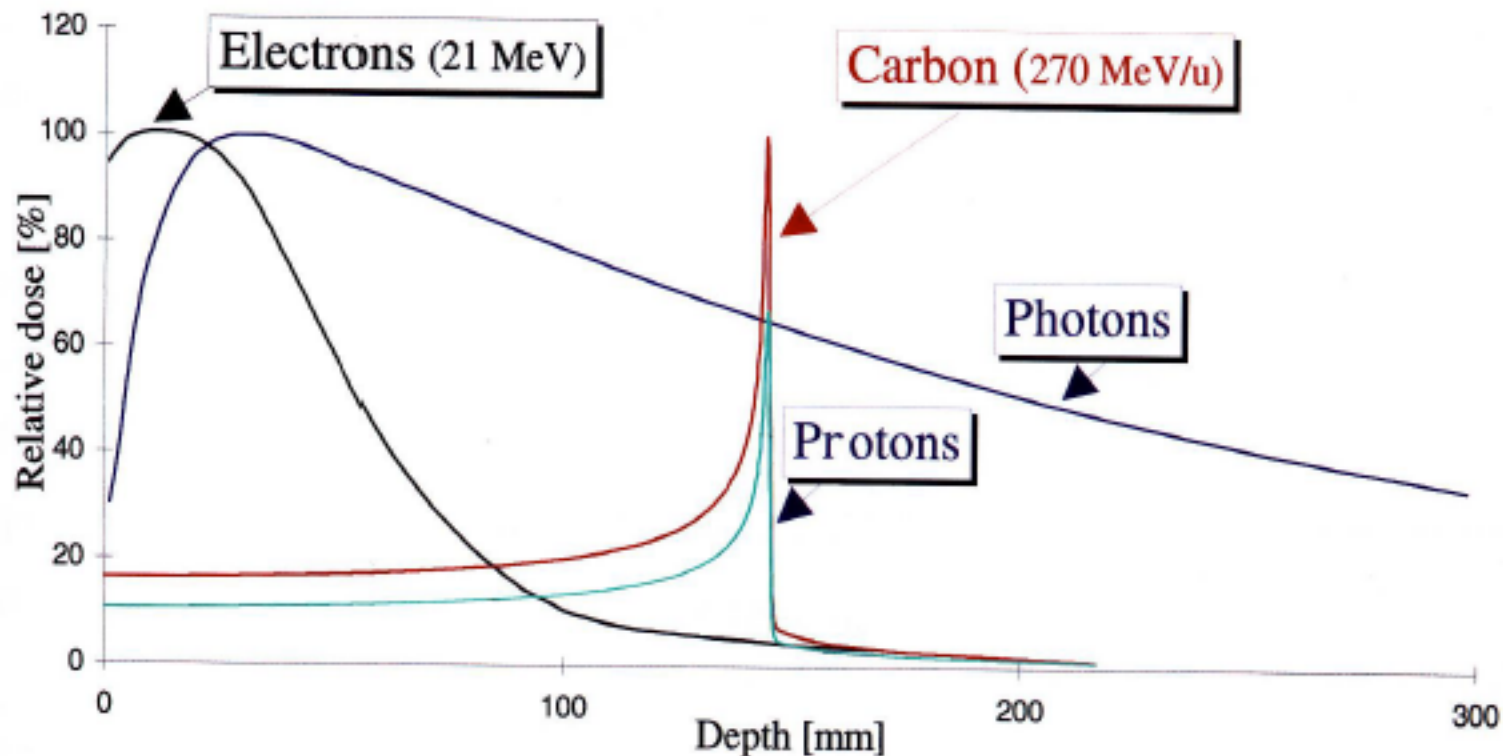
$$\frac{dE}{dx} = Kn_e \frac{Z_{eff}^2}{\beta^2} \left\{ \ln \left[\frac{2m_e c^2 \beta^2}{(1-\beta^2)I} \right] - \beta^2 \right\}.$$



https://upload.wikimedia.org/wikipedia/commons/thumb/2/25/ALICE_TPC_1.jpg/800px-ALICE_TPC_1.jpg

➤ How does the $1/\beta^2$ factor for charged particles work in this formula?

"Bragg Peak": Irradiate only the tumor!



**Manjit Dosanjh, CERN, "Hadron Therapy and European funded projects"
"LHC and beyond" Workshop, St Petersburg, 11 June 2010**

<http://indico.cern.ch/conferenceDisplay.py?confId=89411>

Comparison of DNA damage for gamma rays and charged particles with Bragg peak

DNA

X-rays

Protons

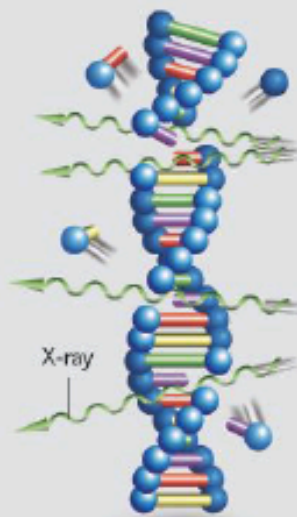
Carbon ions

GREATEST HITS

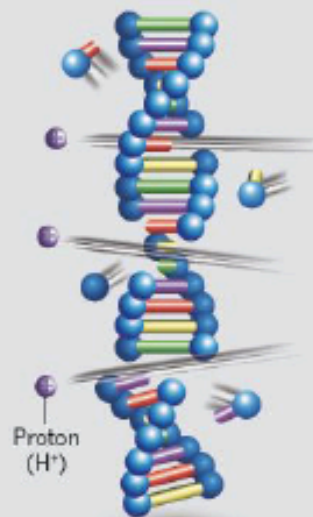
Radiation can kill cancer cells by damaging their DNA. X-rays can hit or miss. Protons are slightly more lethal to cancer cells than X-rays. Carbon ions are around 2–3 times as damaging as X-rays.



DNA

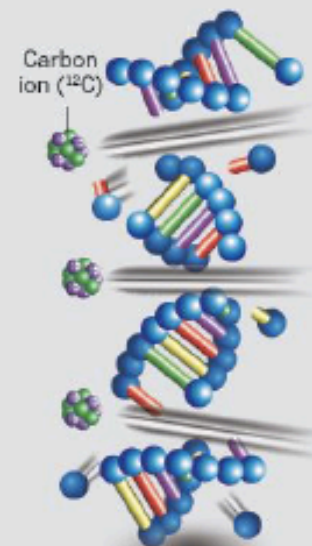


X-ray



Proton
(H⁺)

Proton beam

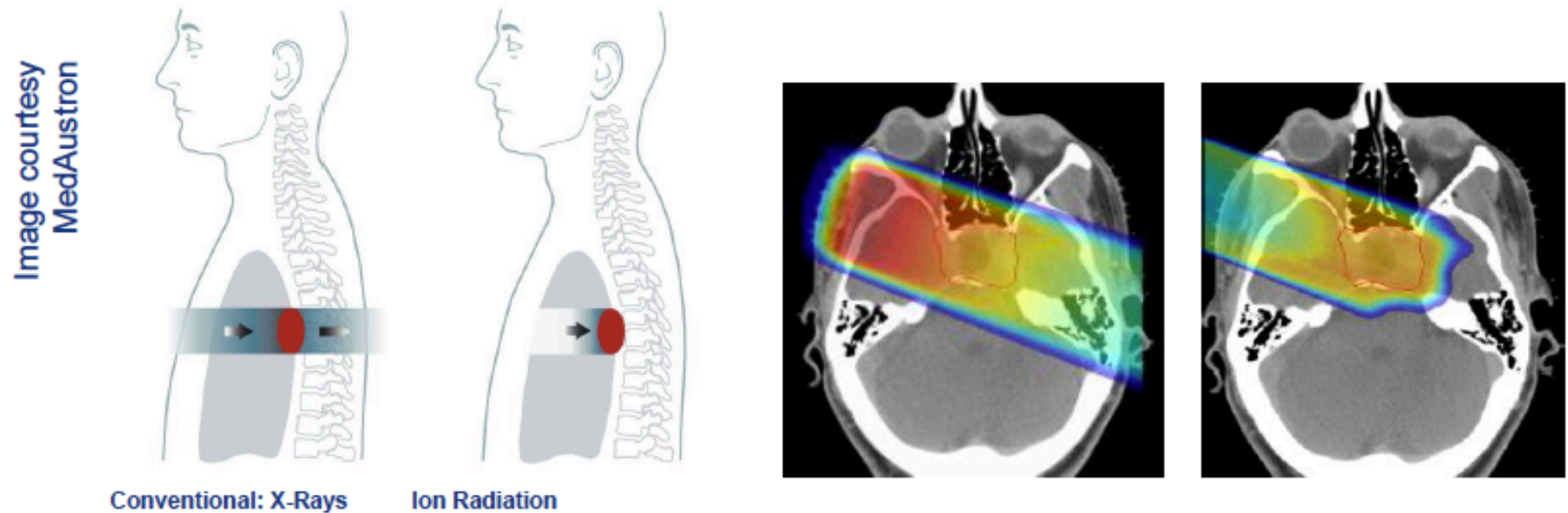


Carbon ion
(¹²C)

Carbon-ion beam

Marx, Nature, 2014

Why is hadron therapy needed?



- During hadron therapy, healthy tissue is practically not irradiated!
- Critical organ could be spared
- See ENLIGHT, <https://enlight.web.cern.ch>

✓ Conclusions

Conclusions

- Global observables in high energy nuclear collisions are defining the base-line platform for interesting physics of HI collisions (including the search for the critical phenomena and study of the nature of quark confinement)
- Instrumentation in fundamental academic studies is bringing always the various spin-offs of very high importance for human society !
(See also the report on Tuesday at 16:00 by Oleg Belov “Applied research with heavy-ion beams”)



Thank you for your
attention!